UNITED NATIONS UNIVERSITY
UNU-GTP
Geothermal Training Programme

Orkustofnun, Grensasvegur 9,
IS-108 Reykjavik, Iceland

Reports 2014
Number 26

PRELIMINARY DESIGN OF A HOT WATER DISTRIBUTION SYSTEM FOR GREENHOUSE HEATING, OLKARIA, KENYA

Felix Kiio Nzioka
Kenya Electricity Generating Company – KenGen
P.O. Box 785 – 20117
Naivasha
KENYA
fnzioka@kengen.co.ke

ABSTRACT

Geothermal energy may be utilized directly or indirectly. Its main use in Kenya is the generation of electricity. Direct utilization of geothermal energy in Kenya is minimal. However, potential direct users are located a few kilometres from the already developed geothermal fields and there is usage potential for a hot water supply for greenhouse heating. Chemistry for re-injection brine has shown that a substantial amount of heat energy may be extracted from the brine without risk of silica scaling. Greenhouse farming requires temperature and humidity control for enhanced plant growth, especially during the night when temperatures are as low as 8°C. Heating domestic water with electricity is expensive in Kenya, therefore utilization of geothermal energy to heat it would be a much cheaper and greener option. Based on the saturation index of silica, the available heat energy of brine from Olkaria North East field is about 16.58 MWt using a mass flow rate of 238 ton/hr. at a supply temperature of 150°C and a return temperature of 90°C. In this study, an evaluation was made on direct use of geothermal energy for one greenhouse complex, one hotel and three residential estates. The study was aimed at coming up with a preliminary design for a hot water distribution system, mainly for greenhouse heating. The design model was generated using the Engineering Equation Solver (EES) software and the design was done as per ASME B31.3-2002 standards. The design considered has a closed loop circuit with heat exchangers at all ends. The total cost of the distribution network is €8,848,000 and the unit cost of heat production is €13.24 per MWh.

1. INTRODUCTION

Direct utilization of geothermal energy in the Olkaria geothermal field in Kenya has not been fully developed. The main focus has been geothermal electricity generation. The field is high-temperature field and liquid-dominated and produces two-phase fluids. Therefore, the mixture is separated before being utilized in power generation. Well site separator stations are located all over the production field and the separated brine is collected for re-injection. The separation occurs at a pressure of about 5 bar and a temperature of about 150°C. The brine has a significant amount of energy that could be extracted before re-injection. Potential applications could be binary electricity generation, greenhouse heating, balneology, industrial processes like drying, and hot water supply to residential areas and hotels. The

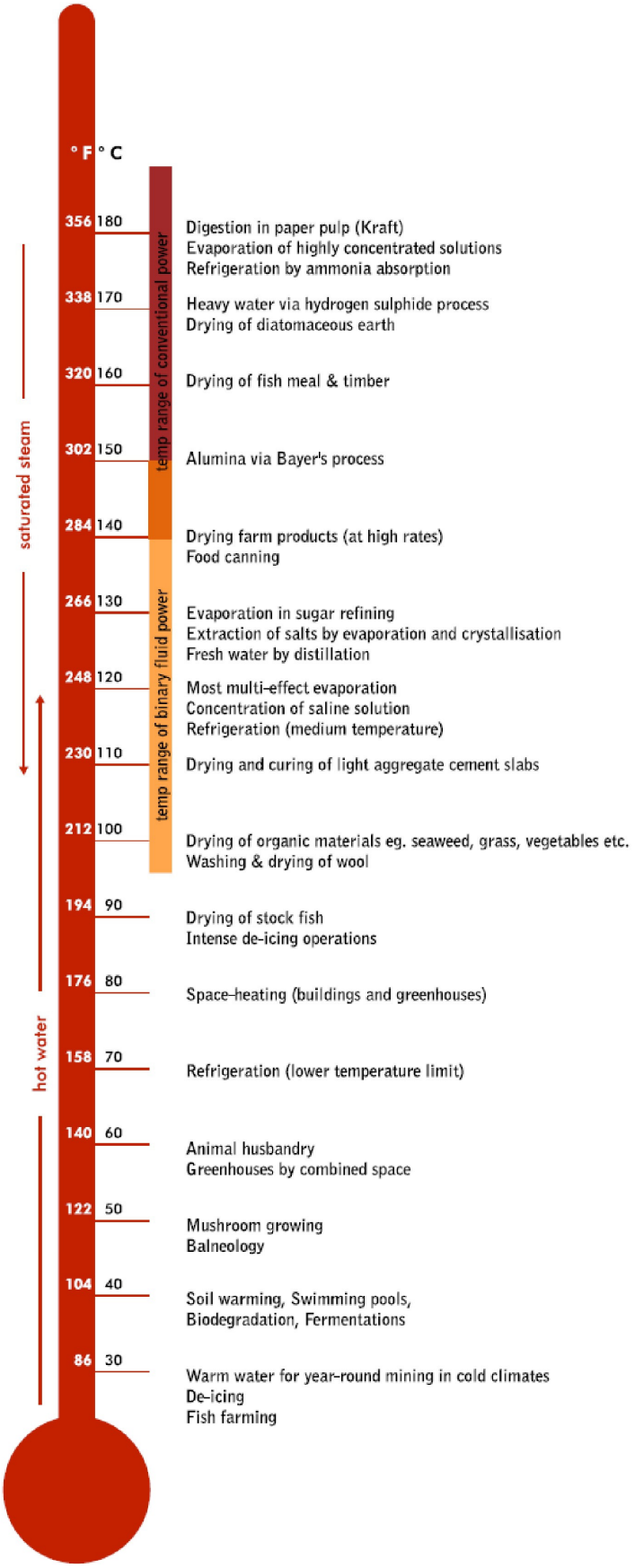

FIGURE 1: Lindal diagram (Líndal, 1973)

brine mass flow rate, for hot re-injection in the Olkaria North East field, is way above 500 t/hr. Electricity generation is the most important form of utilization of high-temperature geothermal resources, while low- to medium-temperature resources are better suited for non-electric applications (Figure 1) (Líndal, 1973). The Lake Naivasha region hosts many flower farming greenhouses, residential estates and hotels which are likely end users of the geothermal energy extracted from brine. The chemistry of the hot brine also determines the extent of the energy extraction. This study presents a preliminary design of a hot water distribution system for greenhouse heating and a hot water supply to residential areas and hotels within the Olkaria geothermal field. This was done by first doing a demand analysis, then transmission pipe design, pumps, heat exchangers and expansion tank sizing.

1.2 Direct utilization in Kenya

A number of direct uses of geothermal energy may be derived from the Lindal diagram (Figure 1). This will vary depending on the available resource. A cascade of direct use applications is possible at the various geothermal fields in the country. The current operational direct utilization of geothermal energy is in greenhouse heating at the Oserian Development Company Ltd (OCDL), Pyrethrum drying, water harvesting in Suswa and Eburru, a spa at Lake Bogoria and the new Olkaria Spa. OCDL has taken the lead in the utilization of geothermal energy for its greenhouses and is utilizing steam from a 1.28 MW well with a total mass flow of 51 t/hr, an enthalpy of 1475 kJ/kg, and an energy equivalent of 15.37 MWt (Lagat, 2010). Two-phase fluid from a well is being used in a heat exchanger to supply hot water to heat 50 hectares of the greenhouses at OCDL (Mburu,

2014). Heating greenhouses helps in temperature and humidity control (Figure 2), thus leading to a reduction in the growth of fungicides. The process of photosynthesis in plants requires carbon dioxide. It is for this reason that OCDL has incorporated a carbon dioxide extraction facility for enhanced plant growth. The carbon dioxide is extracted from the geothermal fluid. Brine sulphur and silica content have balneological effects on the human skin (Mangi, 2013). It is for this reason that the Direct Use and Demonstration Centre (DUDC) in Olkaria was built. The other direct use applications to be demonstrated at the centre include a steam bath, a spa, a sauna, heating and cooling of buildings, hot water supply to residential areas and hotels, fish farming, drying of agricultural produce, greenhouse heating and irrigation (Mangi, 2013). Geothermal energy has also been used directly on a small scale in the drying of pyrethrum at Eburru. Farmers in this area have for decades utilized natural steam at a temperature of 98°C, emitted by fumaroles, to dry their pyrethrum flowers (Lagat, 2010).

FIGURE 2: Greenhouse heating at OCDL (Mangi, 2013)

1.2 Chemistry of Olkaria Northeast brine

The water and the gas chemistry in this field have been analysed in previous studies. Wambugu (1996) found that a hot NaCl type water reservoir exists with temperatures of 270-290°C at depth and major feed aquifers are located below 1300 m depth with a relatively saline fluid (Cl = 300-550 ppm). His study recommended re-injection of brine at temperatures above 170°C in order to avert the possibility of silica scaling. Olkaria Northeast field has a silica concentration of about 500-700 ppm and a pH of about 9 (Mburu, 2010). The wells in this field were connected to the power plant in 2003; brine from the wells is re-injected to four hot re-injection wells, namely wells OW R2, OW R3, OW 703 and OW 708. The mixed brine is monitored on a daily basis before re-injection. Recent predictions of amorphous silica precipitation out of solution, based on data from wells OW R2, OW 703 and OW 708 using the WATCH program, have shown that brine can be re-injected at a temperature of as low as 90°C, without the risk of silica scaling (Figure 3). The WATCH program helps to calculate the aqueous speciation of various components at several pre-determined temperature values for each mineral in order to obtain a log Q/K versus temperature relationship (Mburu, 2010). This study, therefore, considers the use of brine for wells OW 708 and OW R3 which have shown silica precipitation occurring at 90 and 135°C, respectively. Silica precipitation for well OW 703 was found to occur at around 145°C. Sampling data for well OW R2 was not available for the silica modelling. Silica polymerisation and precipitation do not occur at a significant rate until a reasonable degree of super saturation is achieved. Silica scaling problems are not experienced in practice until temperatures rather lower than the theoretical points are reached (Mburu, 2010). A case example from the Berlin geothermal power plant in El Salvador showed that pH adjustment using H_2SO_4 can enable brine to be cooled to lower temperatures without the risk of scaling. Brine pH modification has been shown to be effective and least expensive compared to other inhibitors (Guerra and Jacobo, 2012).

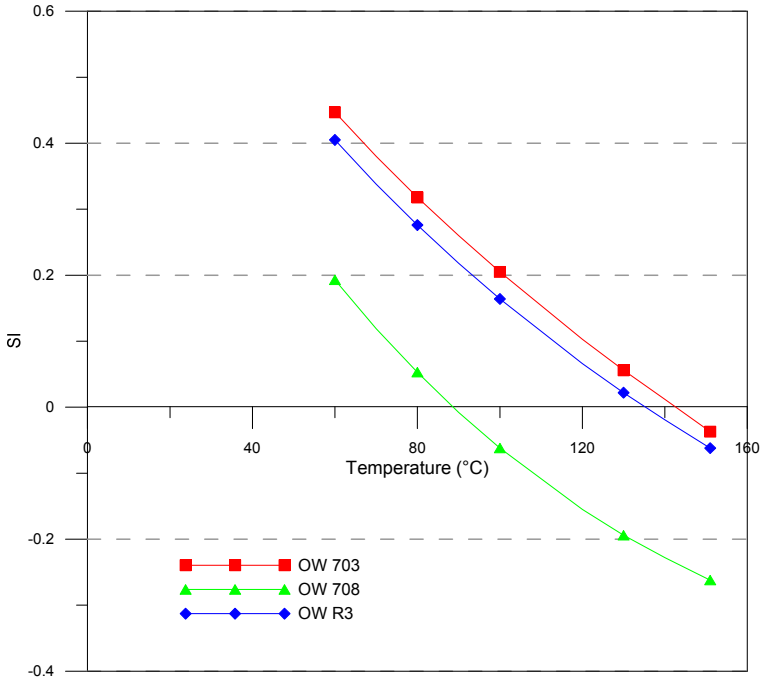

FIGURE 3: Silica Saturation Index (SI) for re-injection brine

FIGURE 4: Pipeline on the surface (modified from Onyango, 2012)

2. PIPELINE DESIGN THEORY

Pipeline design involves several steps outlined in the following sub-sections.

2.1 Route selection

This is a process for identifying constraints, avoiding undesirable areas and maintaining the economic feasibility of the pipeline. Some of the factors that need to be considered are pipeline integrity, cost efficiency, environmental impacts, public safety and land use constraints.

This process involves the use of two methods, i.e. cost modelling comparison, and variable topography distance transforms. Pipelines can either be installed at the surface (Figure 4) or buried underground, where *a* is the horizontal distance between the two pipes and *d* is the depth (Figure 5). In most cases, the distribution of hot water is carried out using buried pre-insulated pipes. This study considers the use a mixture of both buried pipelines and surface pipelines. The method of route selection for this study is based on the total updated cost of the pipeline. Standard distance transform works with a binary digital image that consists of object points and non-object points (Onyango, 2012). The Variable Topography Distance Transform method is used to find optimal paths across physical landscapes for pipelines carrying two-phase geothermal fluid, with the objective of minimizing the capital and operational cost of the pipeline. A distance transform finds the distance from each object point to pixel in an image, and maps the value of the distance to the closest object point (Kjaernested et al., 2013).

2.2 End use demand and flow analysis

Greenhouse farming is a major agricultural activity around Lake Naivasha. Many of the greenhouses major in cut flowers for export. If all greenhouses within a range of 30 km from Olkaria along Moi South Lake Road were heated with geothermal water, then the heat requirement would be enormous, or over 700 MWt (Table 1). The mass flow rate

TABLE 1: Demand analysis

End use	Demand (MWt)
Residential houses	0.19
Hotels	0.05
Greenhouses	752.88
Total	753.12

considered in this study is 238 t/hr at a temperature of 150°C and a pressure of around 5 bar, and has an equivalent heat energy of about 17 MWt. This is the brine meant for re-injection into wells OW 708 and OW R3. Due to the prevailing conditions, only one greenhouse complex, Plantation Plants Kenya Limited, was evaluated for this study. The demand coverage for the greenhouse heating is around 78% of the total area under utilization. Other facilities looped into this distribution system are KenGen housing estates, OrPower housing estate and Fish Eagle inn. BS 6700 (BS, 2006) recommends that the hot water supply to dwellings should be 35-45 litres per person per day; these are the values which were used in the demand analysis for residential areas and hotels. Brine flow rates to re-injection wells in Olkaria North East field are shown in Figure 6. Assumptions made in the analysis include:

a. Greenhouses: minimum temperature required inside greenhouse is 20°C; minimum outside temperature is 8°C; a single plastic sheet is used as the cover material; pipe installation is below the ceiling and on the ground between plots.
b. Residential areas and hotels: Each family house has 6 members and each room has a full capacity of 2 people.

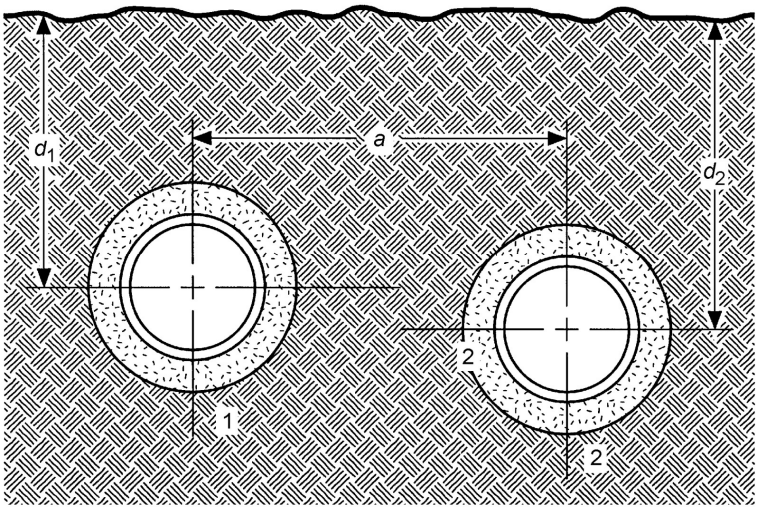

FIGURE 5: Schematic drawing of a pipeline buried underground (ASHRAE, 2008)

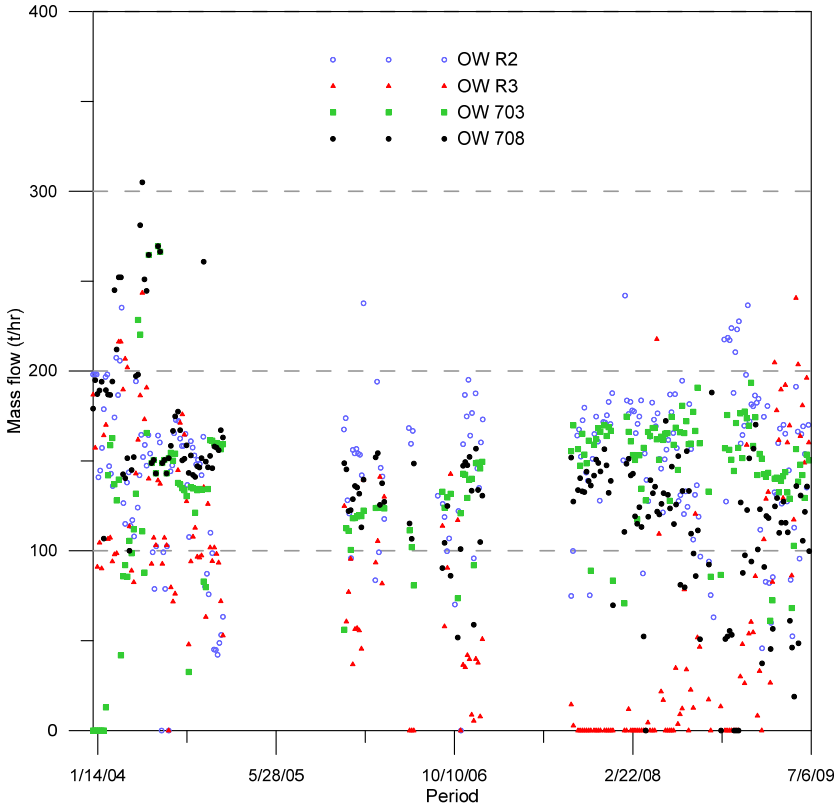

FIGURE 6: Brine mass flow rates to re-injection wells

Heating requirements of the green houses were calculated from the heat losses, Q, in the greenhouse (Equation 1). Heat losses in greenhouses are composed of two components (Panagiotou, 1996):

$$Q = Q_T + Q_I \quad (1)$$

where Q_T = Transmission losses through the roof and the walls (W);
Q_I = Infiltration and ventilation losses due to the heating of cold outside air (W).

Surface areas of the cover materials of the greenhouses were estimated using Google Earth and then combined with the design temperature difference and a heat loss factor (Equation 3) which is the reverse of the overall thermal resistance:

$$Q_T = Q_{Tcover} + Q_{Trest} \quad (2)$$

where Q_{Tcover} = Transmission heat losses through the glazing-covering material (W);
Q_{Trest} = Transmission heat losses through unglazed area (e.g. gutters, frames, masonry) (W).

and

$$Q_{Tcover} = \frac{A_{cover}}{R_{kcover}}(T_i - T_o) \quad (3)$$

where A_{cover} = Glazing area including frames (m^2);
T_i = Indoor temperature (°C);
T_o = Design outside temperature (°C);
R_{kcover} = Overall thermal resistance (m^2 °C/W).

The overall thermal resistance is given by Equation 4. Thermal resistance is dependent on the cover material, wind speed and heating system arrangement in the greenhouse (Appendix I):

$$R_{kcover} = R_{icover} + R_{\lambda cover} + R_{ocover} \quad (4)$$

where R_{icover} = Inside convection resistance (m^2 °C/W);
$R_{\lambda cover}$ = Thermal conductivity resistance [m^2 °C/W);
R_{ocover} = Outside convection resistance (m^2 °C/W).

Neglecting Q_{Trest} in Equation 2, Q_T is approximately equal to Q_{Tcover}, or:

$$Q_T \approx Q_{Tcover} \quad (5)$$

Infiltration losses are analysed by the air exchange method. The number of air exchanges is a function of wind speed, greenhouse construction, and inside and outside temperatures. Therefore Q_I is given by Equation 6:

$$Q_I = \frac{A_{cover}}{R_{vcover}}(T_i - T_o) \quad (6)$$

where R_{vcover} = Thermal resistance for infiltration caused by leaky joints (m^2 °C/W).

The heat energy available in hot water is calculated using Equation 7.

$$Q = mC_p\Delta T \quad (7)$$

where Q = Heat power (W);
m = Mass flow rate (kg/s);
C_p = Specific heat capacity (kJ/kg);
ΔT = Temperature difference (°C).

2.3 Optimization of pipe diameter

The objective of pipe diameter optimization is to minimize the total updated cost based on the pipeline cost, pump station cost, and the annual operation and maintenance cost. According to Jónsson (2014), an increase in diameter increases the capital cost, while the total annual cost decreases and there is an optimum diameter with a minimum total updated cost (Figure 7). However, other factors like the maximum allowable velocity and pressure drop requirements also influence the size of the pipeline.

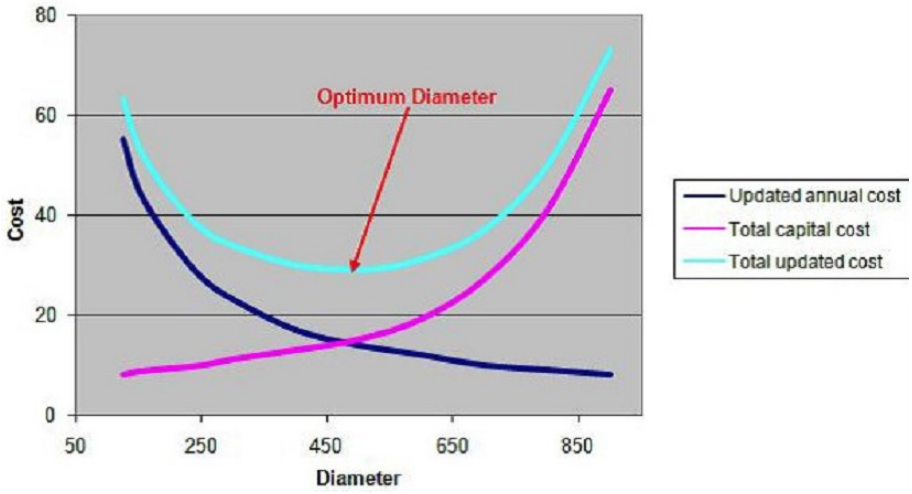

FIGURE 7: Optimum diameter selection based on total updated cost

Therefore, the pipeline should be sized by an economic pressure drop approach. The total updated cost is calculated by Equation 8:

$$C_T = C_c + C_a(1 - \frac{1}{(1+i)^N})/i \tag{8}$$

where C_T = Total updated cost;
C_c = Capital cost;
C_a = Annual operation and maintenance cost;
i = Interest rate;
N = Number of years of operation.

and

$$C_c = L_p c_p + n_b c_b + n_u c_u + n_v c_v + n_{pu} c_{pu} + L_p c_i \tag{9}$$

where L_p = Length of pipe (m);
$c_p, c_b, c_u, c_v, c_{pu}, c_i$ = Cost of pipe, bends, connection units, pumps and pipe insulation, respectively;
n_b, n_u, n_v, n_{pu} = Number of bends, connection units, valves and pumps, respectively.

The cost of other capital items like heat exchangers may be included in Equation 9. Maintenance costs for the distribution network should also be included in the annual cost (Equation 10).

$$C_a = C_{el} O_h P \tag{10}$$

where C_a = Annual operation cost;
C_{el} = Cost of electricity per (kWh);
O_h = Number of annual pump operation hours;
P = Pump power (kW).

The frictional pump power, *P,* is given by Equation 11:

$$P = g\rho H_f Q/\eta \tag{11}$$

where g = Gravitational acceleration (m/s^2);
ρ = Density of fluid, (kg/m^3);
H_f = Frictional head loss (m);
Q = Fluid flow rate, (m^3/s);
η = Efficiency of motor and pump.

Frictional head, H_f (Equation 13), is determined by first calculating the fluid velocity, V, using Equation 12. In order to avoid corrosion, erosion and fluid water hammer in the pipeline, the velocity of the fluid should be kept below 3 m/s for water and 40 m/s for steam.

$$V = Q/A \tag{12}$$

$$H_f = fV^2 l_e/2gD \tag{13}$$

where A = Cross-sectional area of pipe (m^2);
f = Friction factor;
l_e = Second equivalent length of pipeline (m);
D = Inside diameter of pipe (m).

and

$$l_e = l_p + n_b h_b D_{in} + n_c h_c D_{in} + n_u h_u D_{in} + n_v h_v D_{in} \tag{14}$$

where l_p = Length of pipe (m);
D_{in} = Inner diameter (m);
h_b = 20 (Equivalent of bends);
h_c = 20 (Equivalent length of connections, flow through);
h_u = 20 (Equivalent length of expansion units);
h_v = 13 (Equivalent length of gate valves fully open).

The pressure to pump (P_p) is given by Equation 20. The formula for determining the friction factor (f) used in Equation 13 depends on the value obtained for the Reynolds number, R_e (Equation 15), such that:

$$R_e = \rho VD/\mu \tag{15}$$

$$R_e \leq 2100 \tag{16}$$

Then,

$$f = 64/R_e \tag{17}$$

And if,

$$R_e \geq 2100 \tag{18}$$

then,

$$f = \frac{0.25}{\left(Log_{10}\left[\frac{\frac{\varepsilon}{D_{in}}}{3.7} + \frac{5.74}{{R_e}^{0.9}}\right]\right)^2} \tag{19}$$

$$P_p = \left(\Delta Z + H_f\right)\rho g \tag{20}$$

where ε = Absolute roughness (m);
μ = Viscosity (kg/ms);
ΔZ = Elevation difference (m).

2.4 Thickness and pressure class

According to ASME B31.3-2002 (ASME, 2002), the nominal pipe thickness, t_n, should be larger or equal to the requisite pipe thickness, t_m, as shown in Equation 21. The temperature dependent coefficient for steel and other metals can be referenced from the standard for values of thickness lesser than a sixth

of the diameter. The same standard stipulates that the design pressure shall not be less than the pressure at the most severe condition expected during service.

$$t_n \geq t_m = \frac{PD}{\big(2(SE + Py)\big) + A} \tag{21}$$

where P = Design pressure (Pa);
D = Outer diameter (m);
S = Allowable stress (Pa);
E = Welding factor;
y = Temperature dependent coefficient;
A = Additional thickness for milling and corrosion (m).

A pipe having a branch connection is weakened by the opening that must be made in it and, unless the wall thickness of the pipe is sufficiently in excess of that required to sustain the pressure, it is necessary to provide added reinforcements (Figure 8 and Appendix II).

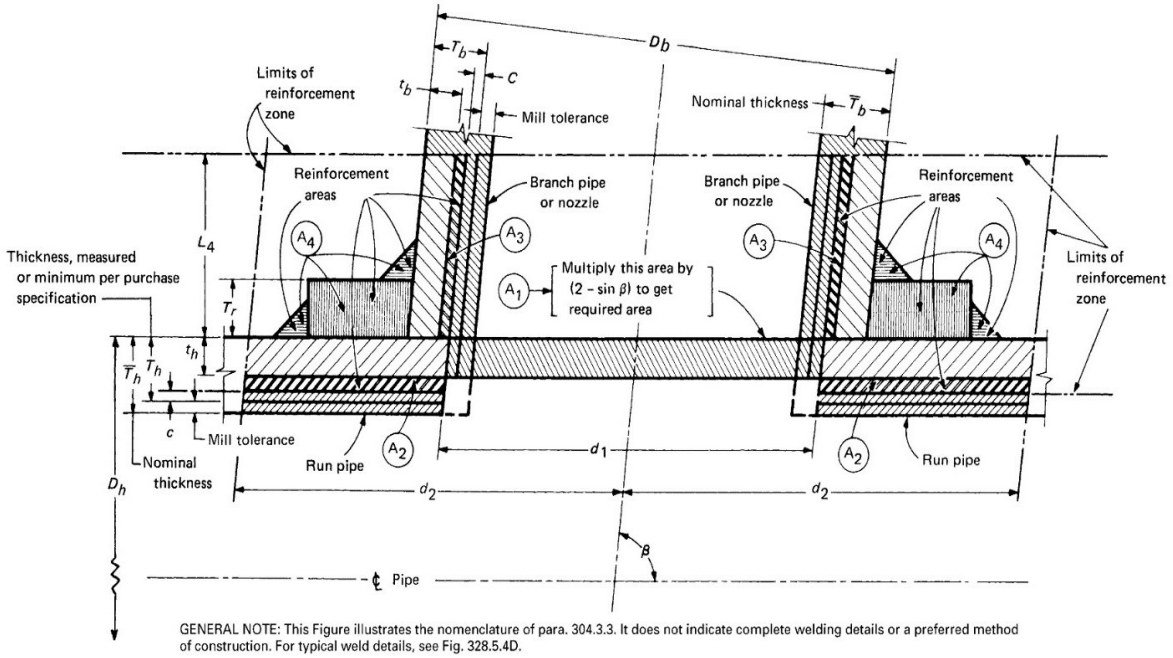

FIGURE 8: Branch connection reinforcement (ASME, 2002)

Reinforcement of branch connections is applicable for connections with a nominal diameter greater than ¼ of the nominal diameter of the run pipe.

$$d_1 = (d_b - 2(T_b - c)/\sin\beta \tag{22}$$

$$d_2 = d_1 \; or \; (T_b - c) + (T_h - c) + d_1/2 \tag{23}$$

$$L_4 = 2.5\,(T_h - c) \; or \; (T_b - c) + T_r \tag{24}$$

$$A_1 = T_h d_1 (2 - \sin\beta) \tag{25}$$

$$A_2 + A_3 + A_4 \geq A_1 \tag{26}$$

where d_1 = Effective length removed from pipe at branch (m);
d_2 = "Half width" of reinforcement zone (whichever is greater, but not greater than the diameter of run/header,D_h) (m);
L_4 = Height of reinforcement zone outside of run pipe (m);

T_b = Branch pipe thickness (measured or minimum per purchase specification) (m);
T_r = Minimum thickness of reinforcing ring or saddle made from pipe (m);
β = Smaller angle between axes of branch and run;
A_1 = Required reinforcement area (m^2);
A_2 = Area resulting from excess thickness in the run pipe wall (m^2);
A_3 = Area resulting from excess thickness in the branch pipe wall (m^2);
A_3 = Area of other metal provided by welds and properly attached reinforcement (m^2).

2.5 Mechanical stress analysis

A pipeline is subject to mechanical and thermal loads during its service life. This may be brought about by the effect of water moving inside the pipeline, thermal gradients and external effects of wind and seismic activities.

2.5.1 Allowable stress

The allowable stress (S) enables the calculation of the length between supports (L_s). The basis for the calculation of the allowable stress (Equation 27) is the yield limit ($R_{p/t}$) and the ultimate stress ($R_{m/T}$) at the calculated temperature. The values of the yield limit and ultimate stress differ from material to material.

$$S = \min\left(\frac{R_{m/T}}{3}, \frac{R_{m/h}}{3}, \frac{2R_{p/c}}{3}, \frac{2R_{p/h}}{3}\right) \quad (27)$$

$$S_h = \min\left(\frac{R_{m/h}}{3}, \frac{2R_{p/h}}{3}\right) \quad (28)$$

$$S_c = \min\left(\frac{R_{m/c}}{3}, \frac{2R_{p/c}}{3}\right) \quad (29)$$

where S_h = Basic allowable stress during hot conditions (Pa);
S_c = Basic allowable stress during cold conditions (Pa).

2.5.2 Sustained and occasional loads

According to the ASME B31.3 standards (2002), the design criteria for the distance between supports requires that the condition stated in Equation 30 be met for sustained loads:

$$\frac{PD_o}{(4t_m)} + (0.75i)\left(\frac{M_A}{Z}\right) \leq S_h \quad (30)$$

where P = Design pressure (Pa);
D_o = Outer diameter (m);
t_m = Minimum thickness (m);
i = Stress intensity factor, where $0.75i \geq 1.0$;
M_A = Sustained bending moment (Nm);
Z = Section modulus (m^3).

Vertical sustained loads q_{sv} are a result of pipe weight, component weight and insulation weight and are calculated using Equations 31 to 33:

$$q_{sv} = q_p + q_e \quad (31)$$

$$q_p = \Pi g \rho_s \left(\frac{\left(D_o^2 - D_i^2\right)}{4}\right) \quad (32)$$

$$q_e = \Pi g \rho_e \left(\frac{(D_e^2 - D_o^2)}{4} \right) \tag{33}$$

where q_p = Pipe weight (N/m);
q_e = Insulation weight (N/m);
ρ_s = Density of steel (kg/m^3);
ρ_e = Density of insulation (kg/m^3);
D_e = Diameter of insulation (m).

The conditions in Equation 33 must be satisfied for occasional loads acting on a pipeline.

$$\frac{PD_o}{(4t_m)} + (0.75i)\left(\frac{M_A}{Z}\right) + (0.75i)\left(\frac{M_B}{Z}\right) \leq kS_h \tag{34}$$

where M_B = Dynamic bending moment (N/m);
k = 1.20, if load is less than 1% of operational time;
= 1.15, if load is active for less than 10% of operational time and;
= 1.0 in other cases.

Vertical occasional loads (q_{ov}, Equation 35) are comprised of the weight of the medium (q_v, Equation 36) being transported, the snow weight (q_s, Equation 37, if applicable), and the seismic vertical load (q_{jv}, Equation 38):

$$q_{ov} = q_v + q_s + q_{jv} \tag{35}$$

$$q_v = \Pi g \rho_v \left(\frac{\left(D_i^2\right)}{4} \right) \tag{36}$$

$$q_s = 0.2SD_e \tag{37}$$

$$q_{jv} = 0.5eq_o \tag{38}$$

$$q_o = q_v + q_p + q_e \tag{39}$$

where S = Snow factor.

The horizontal occasional load (q_{oh}, Equation 40) acting on a pipeline is due to the wind load (q_w, Equation 41) and the horizontal seismic load (q_{jh}, Equation 42):

$$q_{oh} = \max(q_w + q_{jh}) \tag{40}$$

$$q_w = CpD_e \tag{41a}$$

and

$$p = \frac{v^2}{1.6} \tag{41b}$$

$$q_{jh} = eq_o \tag{42}$$

where C = Form factor;
p = Wind pressure;
v = Maximum wind speed (m/s);
e = Seismic factor.

2.5.3 Length between supports

Pipe supports should be located at suitable points so as to support portions of the pipe weight and any other possible loads. The length between the supports should satisfy the conditions stated in Equation 43.

$$L_{sv}^2 \leq \left[kS_h - \frac{PD}{(4t_m)}\right] \frac{\left[\frac{\Pi}{4}(D^4 - d^4)\right]}{\left[D(0.75i)\left\{q_{sv} + (q_{ov}^2 + q_{oh}^2)^{1/2}\right\}\right]} \tag{43}$$

The horizontal length between supports depends upon the expansion arm. The conditions stated in Equation 44 should be met for both vertical constraint(L_{sv}) and horizontal constraint(L_{sh}):

$$\frac{PD}{(4t_m)} + (0.75i)\left\{(q_{sv}L_{sv}^2) + ((q_{ov}L_{sv}^2)^2 + \left(q_{oh}L_{sh}^2\right)^2)^{\frac{1}{2}}\right\}/(8Z) \leq kS_h \tag{44}$$

2.6 Thermal stress analysis

Pipelines transporting hot water are subject to expansion, due to the temperature of the medium being conveyed. This expansion causes thermal stress along the pipeline. If this stress is not addressed and catered for during the design stage, it may lead to failure of the pipeline. It is also a good practise to design for flexibility since the pipe is constrained and its movement should be controlled. Jónsson (2014) suggested that the flexibility may be achieved by the use of expansion loops, expansion units and pre-stressed pipe. Thermal expansion along the pipe is calculated using Equation 45:

$$\Delta L = \propto L\Delta T \tag{45}$$

and thermal strain (ε_X) is given by Equation 46:

$$\varepsilon_X = \frac{\Delta L}{L} \tag{46}$$

where L = Pipe length (m);
$\propto$ = Coefficient of thermal expansion;
ΔT = Temperature difference (°C).

Thermal stress (σ_X) for a pipe with fixed ends is calculated using Equation 47:

$$\sigma_X = E\frac{\Delta L}{L} \tag{47}$$

Expansion loops may be symmetrical (Figure 9a) or asymmetrical (Figure 9b). Symmetrical expansion loops were considered in this study because leg H is used efficiently to absorb an equal amount of

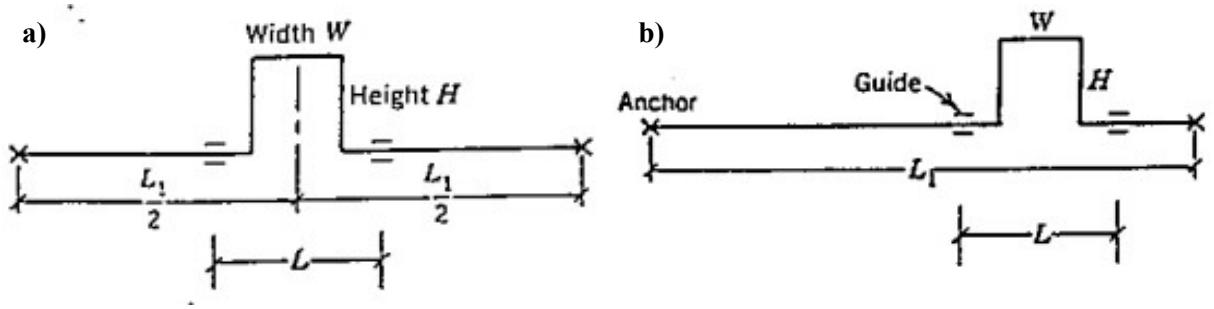

FIGURE 9: Expansion loops; a) Symmetrical; b) Asymmetrical

expansion from both directions (Kannappan, 1986). The total length (L_2) of the expansion loop may be determined from Figure 9a and is given by Equation 48:

$$L_2 = W + 2H \tag{48}$$

The M.W Kellogg chart (Appendix III) was used in the determination of stresses and loads on the expansion loop due to thermal expansion. Legs H and W are determined from Figure 10 and are given in Equations 49 to 50.

$$H = K_2 L \tag{49}$$

$$W = K_1 L \tag{50}$$

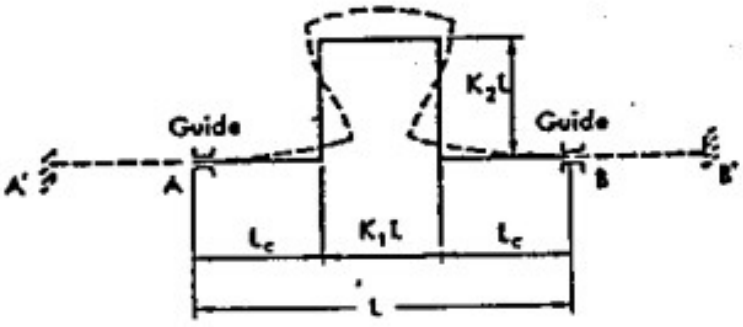

FIGURE 10: Stress and loads in a symmetrical expansion loop

where K_1 and K_2 are constants which can be obtained from the ratios of leg W to the guide distance L, and leg H to the guide distance L, respectively. After using the M.W Kellogg chart to calculate the value of the Y-axis, given by Equation 51, the values of K_1 and K_2 are read from the chart:

$$Y - axis = \frac{L^2 S_A}{10^7 D\Delta} \tag{51}$$

where L = Length from A to B (Figure 10) (m);
S_A = Code allowable stress range;
D = Outside diameter of pipe (m);
Δ = Expansion from A' to B' (Figure 10).

2.7 Pump sizing

Pumps are sized depending on the flow rate required and the height of the lift. The capacity of the pump may be determined from pump curves which are developed by individual pump manufacturers. The curves basically show the performance characteristics based on varying flow rates and head. Pumps may be arranged in parallel or in series, depending on the flow and pressure requirements. The pump power required is also determined by the available static head and friction head, as shown in Figure 11. The frictional head (H_f)is calculated using Equation 13 and the static head is the elevation difference (ΔH)

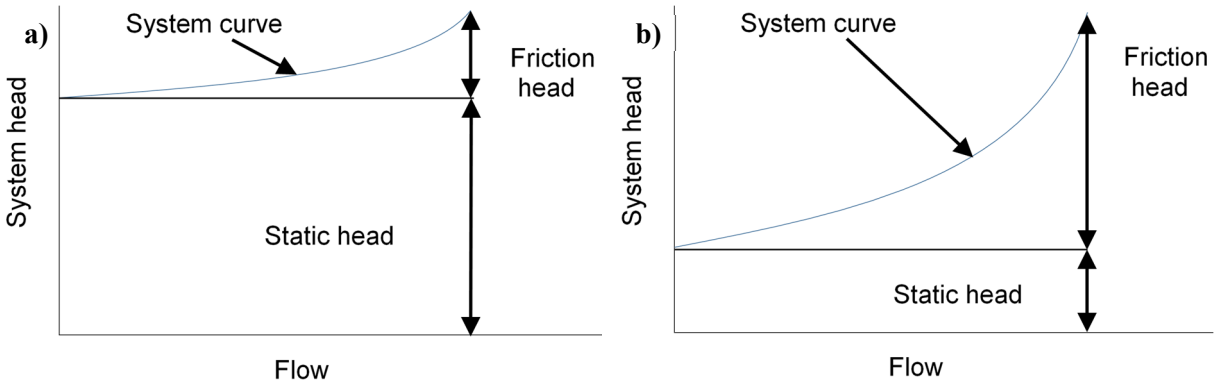

FIGURE 11: System characteristic with, a) Low friction head; and b) High friction head (modified from Jónsson, 2014)

from the lowest point to the highest point; therefore, the total system head (H_T) is given by Equation 52:

$$H_T = \Delta H + H_f \tag{52}$$

The total pump power (P_p) would then be given by Equation 53. Pumps are usually oversized to cater for possible future expansion of the system.

$$P_p = g\rho H_T Q/\eta \tag{53}$$

2.8 Heat exchanger sizing

Heat exchangers may either be of plate type or shell and tube type, and are used for heat exchange between a hot fluid and a cold fluid. Shell and tube heat exchangers are more pressure resistant than the plate type; it is for this reason that shell and tube heat exchangers were chosen for this study. Kakac et al. (2012) suggested a procedure for the design of shell and tube heat exchangers using Logarithmic Mean Temperature Difference (LMTD) method for heat exchanger analysis and includes the following steps:

a. Establish the rate of heat transfer (Q) (Equation 7);
b. Establish the Logarithmic Mean Temperature Difference (LMTD) (Equation 58) and obtain the correction factor (F) if necessary;
c. Calculate the overall duty heat transfer coefficient (U) (Equation 56), assuming fouling to occur on one side;
d. Determine area (A) from Equation 55.

$$Q = UA\Delta T_{lm} \tag{54}$$

$$Q = UAF\Delta T_{lm,cf} \tag{55}$$

$$\frac{1}{U} = \frac{1}{h_i} + R_{fi} + \frac{t}{k} + \frac{1}{h_o} \tag{56}$$

$$F = \phi(P, R, Flow\ arrangement) \tag{57}$$

$$LMTD = \frac{\left(T_{hot,in} - T_{cold,out}\right) - \left(T_{hot,out} - T_{cold,in}\right)}{\ln\left(\frac{\left(T_{hot,in} - T_{cold,out}\right)}{\left(T_{hot,out} - T_{cold,in}\right)}\right)} \tag{58}$$

where ΔT_{lm} = LMTD (°C);
h_i = Inside heat transfer coefficient (W/m^2 K);
h_o = Outside heat transfer coefficient (W/m^2 K);
R_{fi} = Fouling factors;
t = Wall thickness (m);
k = Thermal conductivity (W/m K).

F is non-dimensional and depends upon temperature effectiveness, P, heat capacity ratio R, and the flow arrangement. Equation 54 can be used for multi-pass and cross-flow heat exchangers by multiplying ΔT_{lm}, which would be computed under the assumption of a counter-flow arrangement with a correction factor F as shown in Equation 55. LMTD correction factors for a shell and tube heat exchanger with two shell passes, or four or a multiple of four tube passes (Figure 12), may be obtained from charts in the Tubular Exchanger Manufacturers Association standards (TEMA, 1988).

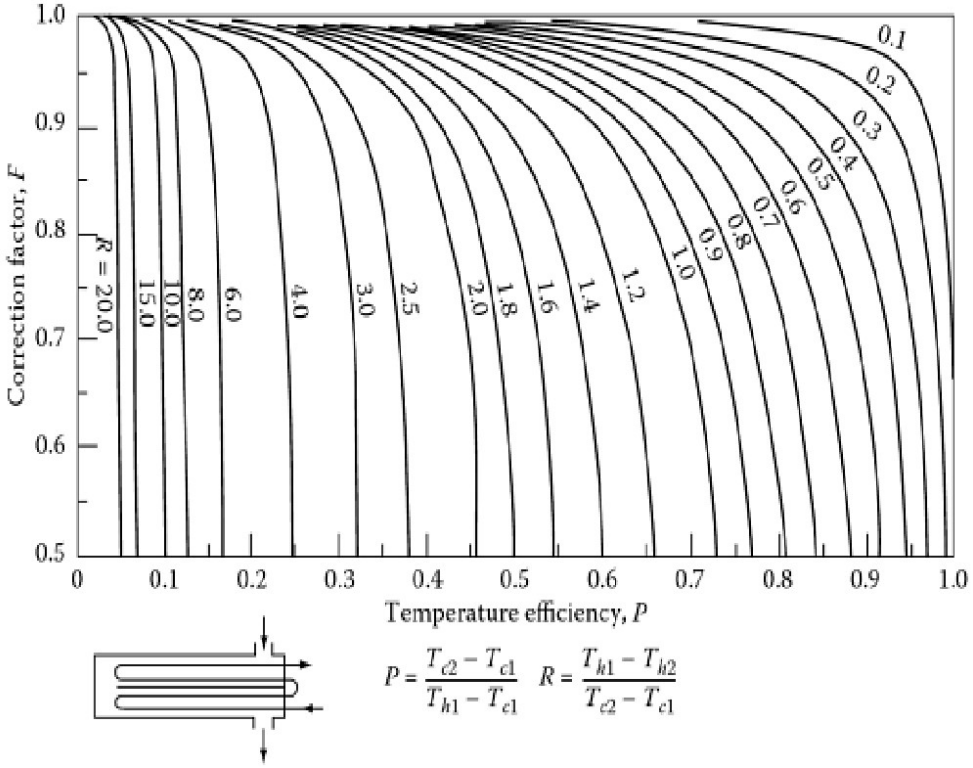

FIGURE 12: LMTD correction factors for a shell and tube heat exchanger with two shell passes, and four or a multiple of four tube passes

2.9 Expansion tank sizing

When cold water is heated up its volume increases; consequently, expansion tanks should be installed in hot water pressurized systems. Expansion tanks may either be pressurized or non-pressurized. The size of a closed expansion tank is determined by the volume of water in the system, system operating temperature, pressures in the system, and the location of the circulation pump. The expansion tank considered for this study is at atmospheric pressure, 30 m above the highest point on the pipeline. The volume of the expanded water (V_{exp}) is calculated using Equation 59; the size of the expansion tank ($V_{exptank}$) is given by Equation 60:

$$V_{exp} = V_p \frac{\rho_c}{\rho_h} \tag{59}$$

$$V_{exptank} = V_{exp} - V_p \tag{60}$$

where V_p = Volume in pipe (m^3);
ρ_c = Density of cold water (kg/m^3);
ρ_h = Density of hot water (kg/m^3).

3. PROPOSED DESIGN OF A HOT WATER DISTRIBUTION SYSTEM

The design consists of a closed loop circuit where water is heated up by the hot geothermal fluid in a shell and tube heat exchanger located at the first pumping station. The reason for this configuration was that the chemistry of the geothermal fluid from the field considered may not allow brine to be cooled below 90°C, without risk of silica scaling in the pipeline and in the re-injection wells. Brine is taken

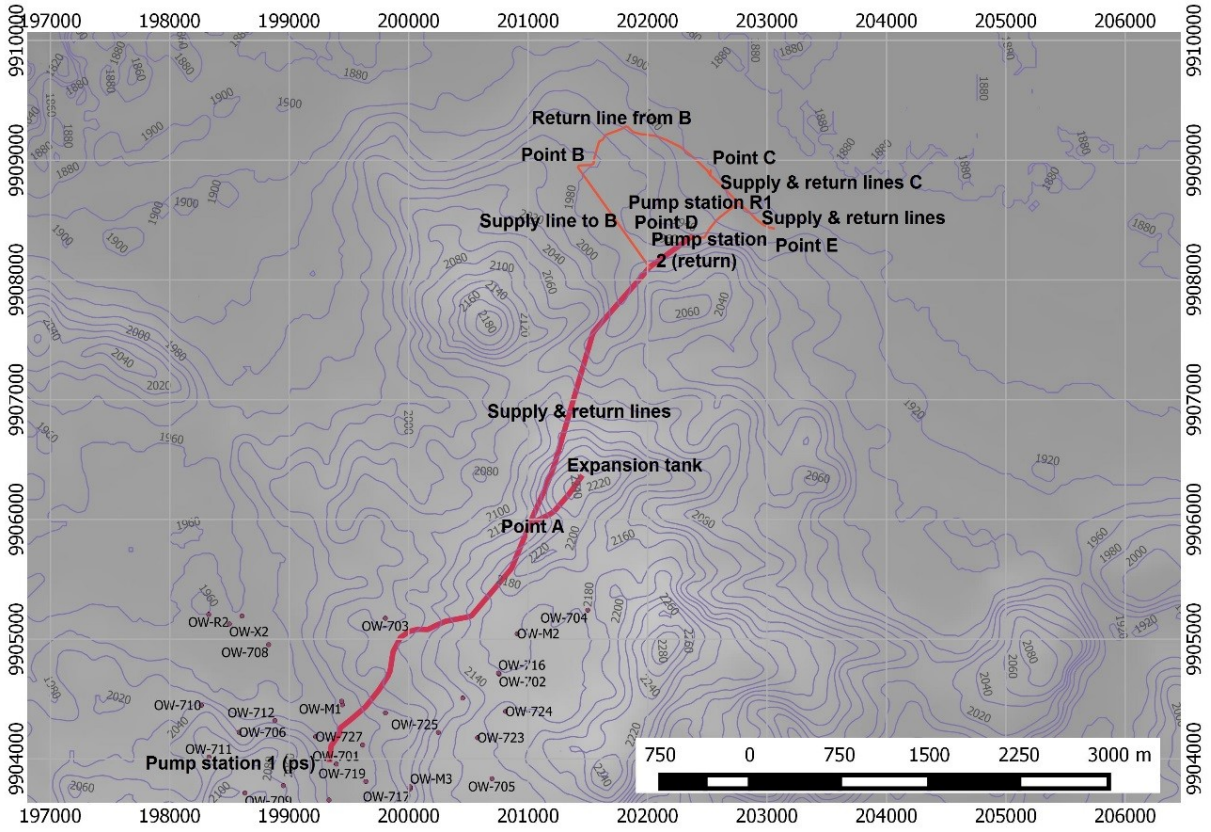

FIGURE 13: Site map showing the proposed flow path

directly from the re-injection line, then into the heat exchanger and back to the re-injection line. The system also has an expansion tank located along the pipeline at a distance of 30 m from the highest point on the pipeline. Make-up water for the main circuit should be topped up at pump station one. The pressure in line A-D is close to 30 bar. Shell and tube heat exchangers were considered at the end use points because they are more pressure resistant than plate type heat exchangers. In less steep areas, the pipeline may be buried underground. The return pipelines from points C, D and E follow the same path as the supply lines, except point B which would require a high-pressure pump capable of overcoming the pressure in the main return line, if the return line was to follow its supply line path. Therefore, the return flows to return line pumping station R1 (Figure 13). A schematic diagram of the proposed system is shown in Figure 14. An open loop circuit could have been considered as well, but this would have involved the setting up of a new water supply line and a water treatment plant, which could further increase the cost.

3.1 Design data

The pipeline is assumed to follow the already existing roads for ease of installation and maintenance. Figure 13 shows the site map with the proposed flow path. Pump station one is assumed to be located as near to the brine re-injection line as possible. Main supply and return lines are assumed to follow the same path, however, the return line from point B goes down the hill to connect with return lines from points C and E at return line pump station R1. The specifications for pipeline material, heat exchanger materials and expansion tank material used in this study are listed in Table 2. Polyurethane/Polyisocyanurate (PUR/PIR) insulation material may offer optimal insulation solution, compared to other insulation materials, due to their low thermal conductivity values and long term performance. Polyisocyanurate (PIR) has a higher hot surface performance temperature of 150°C while that of Polyurethane (PUR) is 110°C (Table 3). These insulation materials are CFC free and are suitable for large diameter pipelines, underground pipes and storage tanks (NGP Industries, 2014). Therefore, PIR pre-insulated insulated pipeline was selected for this study.

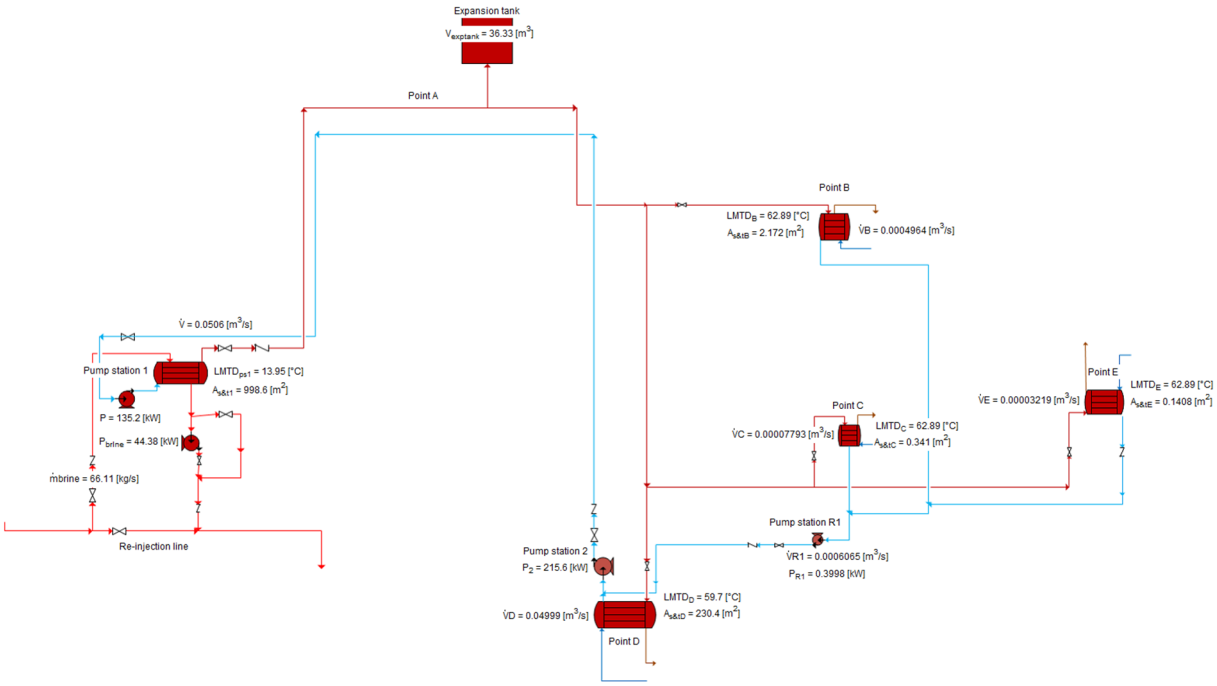

FIGURE 14: Schematic diagram of the distribution network

TABLE 2: Materials

Material	Type
Pipe material (pre-insulated)	S235
Heat exchanger tubes	SS316
Heat exchanger shell	S235
Insulation material	PIR

TABLE 3: Technical specifications for PUR/PIR insulation materials

Properties	Polyisocyanurate (PIR)	Polyurethane foam (PUR)
Density	32 ± 2 Kg/m³	36 ± 2 Kg/m³
Compression strength	172 KN/m²	172 KN/m²
Thermal conductivity	Max 0.021 W/mk	Max 0.021 W/mk
Temperature limit	+ 150-200°C	+ 110-180°C

Mean monthly values for weather data recorded from the Naivasha meteorological station (Mpusia, 2006) are shown in Figure 15. The mass flow rates for brine to the four hot re-injection wells in the Olkaria North East field are shown in Figure 6. Due to the limited available resource capacity, the entities shown in Table 4 were considered for this study. The maximum mean wind speed value from Figure 15 is 1.5 m/s. Typical values for overall duty heat transfer coefficient in shell and tube heat exchangers were referenced from Cheremisinoff and Cheremisinoff (1995). Branch connection pipes

TABLE 4: Sustainable demand

End use	Entity name	Point	Altitude (m)	Demand (MWt)
Residential houses	Kengen	B	1984	0.16
Residential houses	Orpower	C	1904	0.03
Hotels	Fish Eagle Inn	E	1906	0.01
Greenhouses	Plantation plants K, Ltd.	D	1946	16.37

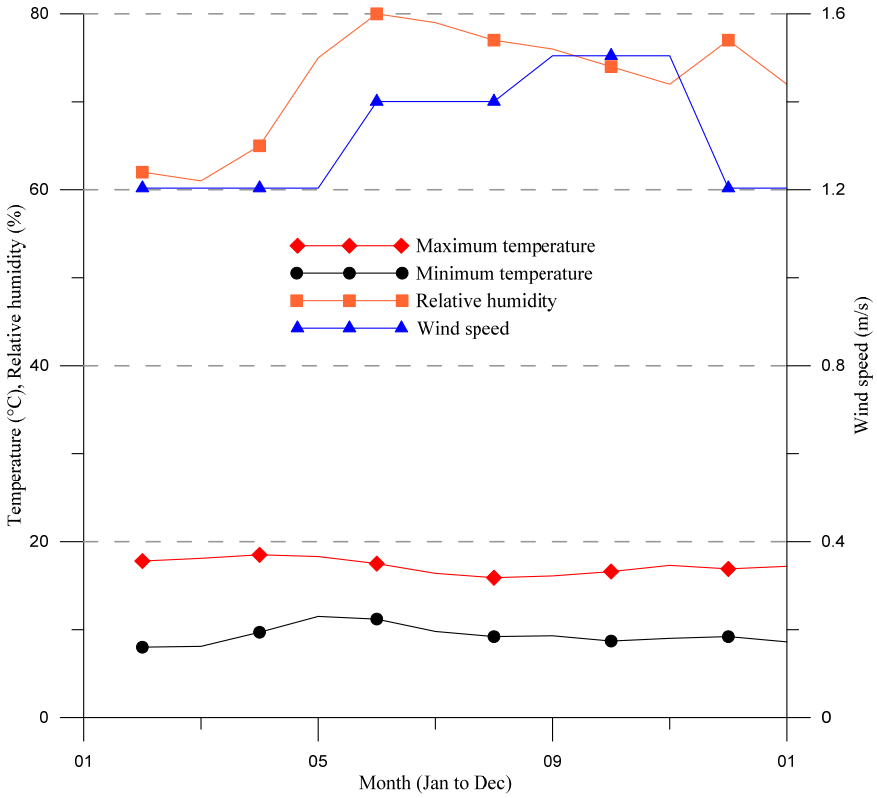

FIGURE 15: Mean monthly values for weather data in Naivasha

diameters were referenced from ASTM F681 – 82, (ASTM, 2008) (Standard practice for use of branch connections for fabricated joint, cut-in branch). The retail cost of electricity for industrial consumers of 0.072 USD/Kwh was picked from Kinyanjui et al. (2011). The altitude above sea level at pump station one is 2015 m, at pump station two it is 1946 m, at pump station R1 1901 m, and at point A 2211 m.

3.1.1 Assumptions

The assumptions made in the design are listed below:

a. SI units were used in all calculations;
b. Elevations of the various points were picked from Google Earth;
c. Insulation thickness of 0.050 m;
d. Additional thickness for milling and corrosion of 0.0015 m;
e. Seismic factor of 0.24 for Olkaria;
f. Pipe bend at every 60 m;
g. Main circuit supply temperature of 145°C and a return temperature of 60°C;
h. Combined motor and pump efficiency 77%;
i. Cost of pipeline is in €/m and expansion tank is in €/m^3 and are picked from cost of projects currently being handled by VERKIS Consulting Engineers, Iceland;
j. Cost of pipe fittings, bends, pipe supports and civil works is included in the cost of pipeline;
k. Cost of pump is in €/kW and includes cost of pump station house, piping and pump controls system;
l. Cost of heat exchangers is in Euro/m^2 and is based on a study done by Reykjavik Energy;
m. Cost of buried pipe to be equal to cost of above surface pipe;
n. Cost uncertainty at this stage of design is estimated to be 20%;
o. Cost of design and supervision 10%;
p. Operation and maintenance cost: 4% for pumps and machinery with moving parts, 1% for pump stations civil structures and piping: 2% for heat exchangers: and 1% for rest of pipeline;
q. Interest rate 6%;
r. Distribution system life span of 30 years.

3.2 Results

The design model was generated from Engineering Equation Solver (EES) (see Appendix IV). From the model, two paths, A and B, were evaluated. The path with the lowest total updated cost was path A, as shown in Table 5; therefore, it was selected as the best path. The design of the system was done as per ASME B31.3 (2002). The design pressure for line ID Ps-A was 18 bar, while that of line ID A-D was 24 bar; therefore, pipes with pressure class PN 40 were selected. The allowable stress for hot conditions was 113 Mpa. The requested thickness obtained was 0.004 m and, comparing it with the nominal thickness of 0.005 m, satisfied the ASME B31.3 (ASME, 2002) condition for thickness and pressure class. The length between supports was 3.2 m; this condition was met. The results of the main circuit supply pipeline configuration are shown in Table 6, while those of the return pipeline are shown in Table 7. The results of the heat exchangers, expansion tank and pumping stations are shown in Table 8. An optimum pipe diameter for the main circuit supply and return lines was selected, after carrying out minimization of the total updated cost using different pipe diameters ranging from DN 100 to DN 500 with PN 40 as the pressure class. The pipe diameter which gave the lowest total updated cost is DN 200, as shown in Figure 16. From experience, it has been proven that the pressure drop in long pipelines should be around 10 mm/m; therefore, DN 200 was selected as the pipe diameter, satisfying all conditions by having a fluid velocity of 1.5 m/s, and a pressure drop of 13 mm/m.

TABLE 5: Route selection

Path	Description	Length supply pipe (m)	Length return pipe (m)	Diameter (mm)	Total updated cost (€)
A	Pump station across hill-point D	5610	5610	200	19,880,000
B	Pump station Olkaria road-point D	10200	10200	200	26,600,000

TABLE 6: Main circuit supply pipe line

Line ID	Length (m)	Diameter (mm)	Unit cost (€/m)	Cost (€)
Brine pipe	200	200	344	68,800
Ps - A	2400	200	344	825,600
A - D	3210	200	344	1,104,240
Expansion Tank connection pipe	457	200	344	157,208
Branch connection B	1260	100	180	226,800
Branch connection C	444	65	70	31,080
Branch connection E	474	65	70	33,180
Total				**2,446,908**

TABLE 7: Main circuit return pipe line

Line ID	Length (m)	Diameter (mm)	Unit cost (€/m)	Cost (€)
E-D	474	65	70	33,180
D-Ps	5610	200	344	1,929,840
Branch connection C, return	444	65	70	31,080
Branch connection B, return	1770	100	180	318,600
Return pipe R1	646	40	43	27,778
Total				**2,340,478**

TABLE 8: Heat exchangers, expansion tank and pumps

Item	Size	Unit	Unit cost (€/unit)	Cost (€)
Heat exchanger at ps1	998.6	m^2	500	499,300
Heat exchanger at B	2.172	m^2	500	1,086
Heat exchanger at C	0.341	m^2	500	170
Heat exchanger at D	230.4	m^2	500	115,200
Heat exchanger at E	0.1408	m^2	500	70.4
Expansion tank	36.33	m^3	500	18,165
Pump station 1, pump 1	135.2	kW	3500	473,200
Pump station 1, pump 2	44.38	kW	3500	155,330
Pump station R 1	0.3998	kW	3500	1,399
Pump station R 2	215.6	kW	3500	754,600
Total				**2,018,521**

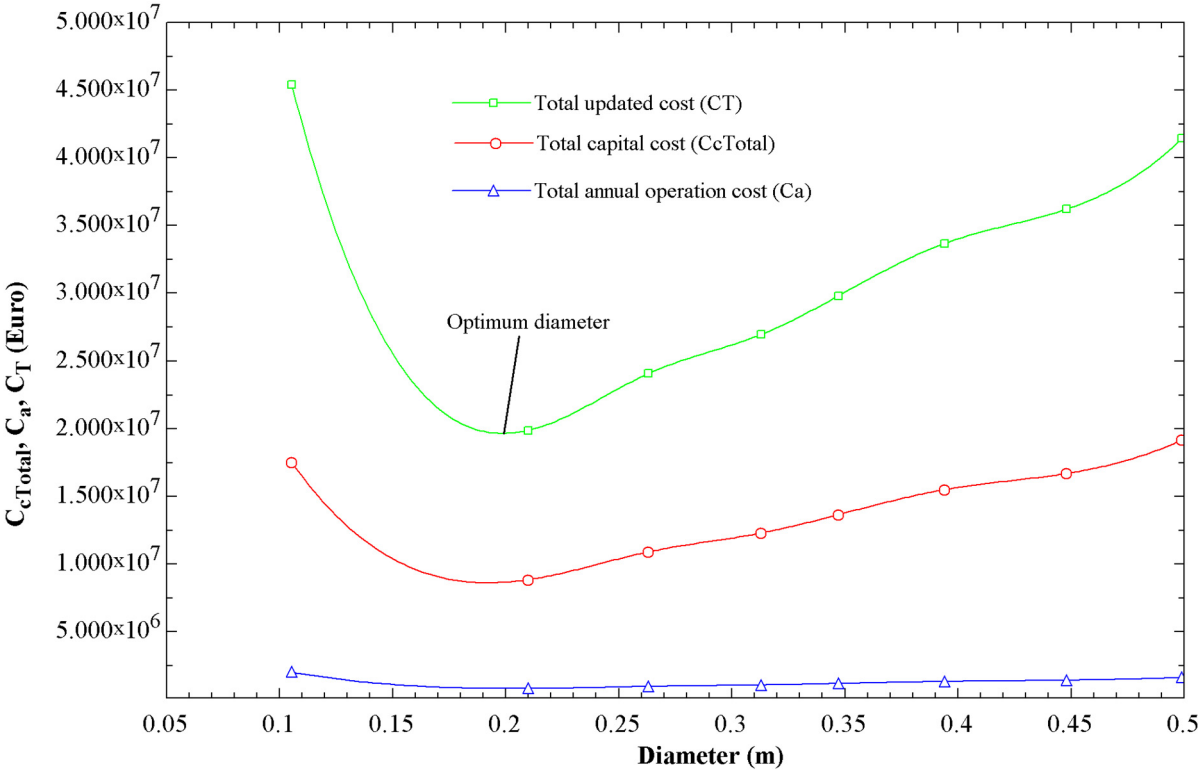

FIGURE 16: Optimum diameter selected based on minimum total updated cost

The total cost for the main circuit supply pipeline is €2,446,908 and for the return pipeline is €2,340,478. The total cost for the pumping stations is €1,384,529, for the heat exchangers is €615,827, and €18,165 for the expansion tank. The subtotal for the project is €6,805,907. Additional costs include € 680,591 for design and supervision, and € 1,361,181 for uncertainty (Figure 17). The grand total cost for the whole project is € 8,847,679.

3.3 Production cost analysis

The total project cost was further used to project the cost of heat per MWh. Annual operation and maintenance cost were calculated by the model developed in EES, as shown in Table 9. The maximum number of hours for full capacity operation was taken to be 10 hours per day, giving an annual

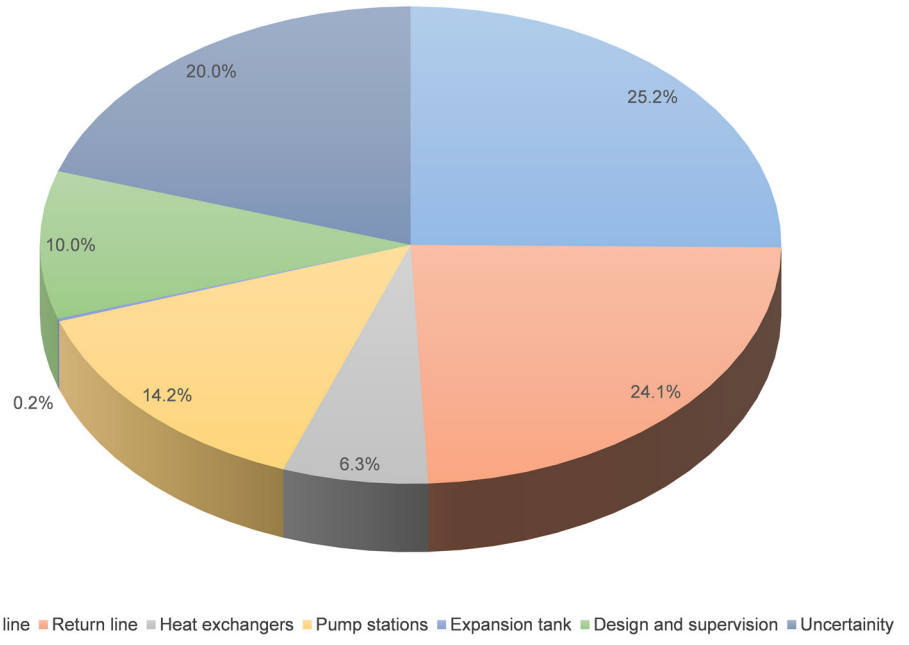

FIGURE 17: Percentage distribution of project cost

production of heat of 60,520 MWh/year. The heating capacity used is 16.58 MWt. The unit production cost of heat obtained is 13.24 €/MWh.

TABLE 9: Production cost

Item	Cost, €	Remarks
Capital cost		
Pipeline	4,787,386	Inclusive of pipe fittings, bends, insulation, valves, pipe supports and civil works
Heat exchangers	615,827	
Pump stations	1,384,529	Inclusive of pumps, controls, piping and civil structures
Expansion tank	18,165	Inclusive of construction materials and civil works
Design and supervision	680,591	
Uncertainity	1,361,181	
Total capital cost	8,847,679	
Annual operation and maintenance cost		
Pumps and moving parts	5,537	4% of pump and moving parts cost (about 10% of pump station cost)
Pump station pipi. & civil struct.	12,459	1% of pump station cost
Heat exchang. & expansion tank	12,317	2% of total hx cost
Main pipeline	48,056	1% of pipeline cost
Cost of capital, PMT	642,755	I is 6% and N is 30 years
Cost of electricity	80,035	10 h. daily operation, 0.072 USD/kWh which is equivalent to 0.0544 €/kWh at exchange rate of 1 USD=0.77 €
Total annual cost	801,158	
Capacity for heating, MWt	16.6	
Duration operation, oh, h./year	3650	10 hours of operation per day
Annual production of heat, MWh/year	60,520	
Unit production cost heat, kWh	1.354	€cents/kWh
Unit production cost of heat, MWh	13.24	€/MWh

4. CONCLUSIONS

The available energy extractable from geothermal brine from the North East field may not be adequate to satisfy heating requirements for all greenhouses within 30 km from Olkaria. The available resource may only satisfy 78% of the total heating requirements for the selected greenhouse complex. However, the resource may fully satisfy the hot water supply requirements for the three housing estates and one hotel considered in the study.

The results of the route selection showed that route A has the least total updated cost, compared to route B, and was therefore selected as the best route.

The results for diameter optimization showed that the suitable pipeline for the distribution network should have a diameter of DN 200 with a pressure class PN 40. The pressure drop obtained for the distribution network was 13 mm/m, and a fluid velocity of 1.5 m/s. The ASME B 31.3 (ASME, 2002) conditions for thickness and pressure class, length between supports and allowable stress were all satisfied.

A closed loop heating system is more suitable than an open loop system, due to the limitations of silica scaling. The shortest distance to the greenhouse complex considered in the study is around 5.6 km across the hill. The total capital cost for the distribution network is € 8,847,680, thus placing the unit production cost of heat at 13.24 €/MWh.

ACKNOWLEDGEMENTS

I thank the UNU-GTP management, especially the Director, Mr. Lúdvík S. Georgsson, for the opportunity to attend the 2014 fellowship programme. My acknowledgement also goes to my project supervisor, Mr. Óskar Pétur Einarsson of VERKÍS Consulting Engineers, for his continuous guidance and assistance in the project work. I also thank Mrs. María S. Gudjónsdóttir, Ms. Málfrídur Ómarsdóttir, Mr. Ingimar G. Haraldsson, Mr. Markús A.G. Wilde and Ms. Thórhildur Ísberg, for their support throughout the entire training period. I also thank my fellow colleagues, who offered support in one way or another. My special thanks go to my employer, KenGen, for nominating me to attend the UNU-GTP programme.

I appreciate my family, Thecla and Ryan, for the moral support they gave me during the entire training period. My deepest thanks goes to the Almighty God for enabling me to successfully complete the training.

REFERENCES

ASHRAE, 2008: *District heating and cooling*. American Society of Heating, Refrigerating and Air-Conditioning Engineers (ASHRAE) Inc., Atlanta, GA, 355 pp.

ASME, 2002: *ASME code for pressure piping*. ASME B31.3–2002, revision of ASME B31.3-1999.

ASTM, 2008: *Standard practice for use of branch connections.* ASTM F681 – 82.

BS, 2006: *Design, installation, testing and maintenance of services supplying water for domestic use within buildings and their curtilages – Specification.* BS 6700:2006 (3rd edition).

Cheremisinoff, P.N., and Cheremisinoff, N.P., 1995: *Process engineering data book*. Technomic Publishing Co., Inc., Lancaster, PE, 345 pp.

Guerra G., C.E., and Jacobo P.E., 2012: pH modifications for silica control in geothermal fluids. *Presented at "Short Course on Geothermal Drilling, Resource Development and Power Plants", UNU-GTP and LaGeo, San Salvador, El Salvador,* 9 pp.

Jónsson, M.Th., 2014: *Pipe design*. UNU-GTP, Iceland, unpublished lecture notes.

Kakac, S., Liu, H., and Pramuanjaroenkij, A., 2012: *Heat exchangers selection, rating and thermal design*. Taylor and Francis Group, NY, USA, 150 pp.

Kannappan, P.E.S, 1986: *Introduction to pipe stress analysis*. John Wiley & Sons, Inc., NY, 255 pp.

Kinyanjui, B., Kibiru, G., Wasioya, B., Kiruja, E., Akuto, S., Simiyu, T., Nabaala, A., Mungai, K., Mabea, G., Mworia, B., Karembu, A., Kariuki, D., Kariuki, G., Cheboi, S., Kirui, S., Musyoka, B., Njeru, G., Njiraini, W., 2011: *Updated least cost power development plan, study period: 2011-2031.* Republic of Kenya, 203 pp.

Kjaernested, S.N., Jónsson, M.T., Pálsson, H., 2011: A methodology for optimal geothermal pipeline route selection with regards to visual effects using distance transform algorithms. *Proceedings of the 36th Workshop on Geothermal Reservoir Engineering, Stanford, CA,* 10 pp.

Lagat, J., 2010: Direct utilization of geothermal resources in Kenya. *Proceedings of the World Geothermal Congress 2010, Bali, Indonesia*, 7 pp.

Líndal, B., 1973: Industrial and other applications of geothermal energy. In: Lund et al. (2005), *World-wide direct uses of geothermal energy. Proceedings of the World Geothermal Congress 2005, Antalja, Turkey*, 20 pp.

Mangi P., 2013: Direct utilization in Kenya – A case of geothermal spa and demonstration centre at Olkaria, Kenya. *Presented at "Short Course VIII on Exploration for Geothermal Resources", UNU-GTP, KenGen and GDC, Naivasha, Kenya*, 14 pp.

Mburu M., 2010: Feasibility study on direct utilization of energy from geothermal brine - a case study of Olkaria geothermal power plant, Kenya. *Proceedings of the World Geothermal Congress 2010, Bali, Indonesia*, 9 pp.

Mburu M., 2014: Geothermal energy utilization at Oserian flower farm Naivasha, Kenya. *Presented at "Short Course VI on Utilization of Low- and Medium-Enthalpy Geothermal Resources and Financial Aspects of Utilization", organized by UNU-GTP and LaGeo, Santa Tecla, El Salvador*, 6 pp.

Mpusia, P.T., 2006: *Comparison of water consumption between greenhouse and outdoor cultivation*. International Institute for Geo-Information Science and Earth Observation, Enschede, Netherlands, MSc thesis, 86 pp.

NGP Industries, 2014: *Technical specifications for PUF/PIR pipe sections.* NGP Industries Ltd., webpage: www.ngpil.com/puf_products.php.

Onyango S.O., 2012: Preliminary design of the Menengai phase I steam gathering system. Report 26 in: *Geothermal training in Iceland 2012*. UNU-GTP, Iceland, 601-641.

Panagiotou, C., 1996: Geothermal greenhouse design. Report 11 in: *Geothermal training in Iceland 1996*. UNU-GTP, Iceland, 219-250.

TEMA, 1988: *Standards of the tubular exchanger manufacturers association.* TEMA.

Wambugu J.M., 1996: Assessment of Olkaria North-East geothermal reservoir, Kenya, based on well discharge chemistry. Report 20 in: *Geothermal training in Iceland 1996*. UNU-GTP, Iceland, 481-509.

Appendix I: Greenhouse thermal resistance values (modified from Panagiotou, 1996)

Thermal resistance		$m^2°C/W$
Greenhouse thermal resistance caused by air infiltration, R_{vcover} (DN 4701)	*Cover material* Glass in putty Plastic film greenhouse Plastic tent (tunnel) Putty less glazing in metal frame with rubber gaskets	 1.0 2.0 2.0 1.0
Greenhouse thermal resistance by conduction, $R_{\lambda cover}$ (DN 4701)	Single glass Plastic panel corrugated GFK 1 mm Double glass in steel frame Space 15 mm Space 12 mm Space 6 mm Double poly frameless Space 12 mm Space 5 mm Double plastic film, space 10 mm Single plastic film (PVC, PE) thickness of 0.2 mm	0.01 0.01 0.14 0.11 0.09 0.15 0.08 0.10 0.01
Greenhouse thermal resistance by outside convection, R_{ocover}, as a function of wind speed (DN 4701)	*Wind speed (m/s)* 1 2 3 4 5 6 7 8 9 10	 0.102 0.0725 0.0562 0.0459 0.0388 0.0307 0.0346 0.0277 0.0252 0.0232
Greenhouse thermal resistance by inside convection, R_{icover} (DN 4701)	*Heating system* Pipes suspended from the ceiling Pipes on the walls Pipes under the raised tables Pipes on the floor between plots Fan coil units Unit heaters Finned pipes Combination of the above	 0.09 0.09 0.01 0.12 0.09 0.01 0.09 0.1

APPENDIX II: ASTM F681 – 82 (2008) Branch connection matrix for carbon steel piping (Key: 1 = Tee or lateral butt weld, 2 = Tee or lateral socket weld or threaded, 3 = Welded outlet butt weld end, 4 = Welded outlet socket weld or threaded end, 5 = Fabricated joint cut-in branch)

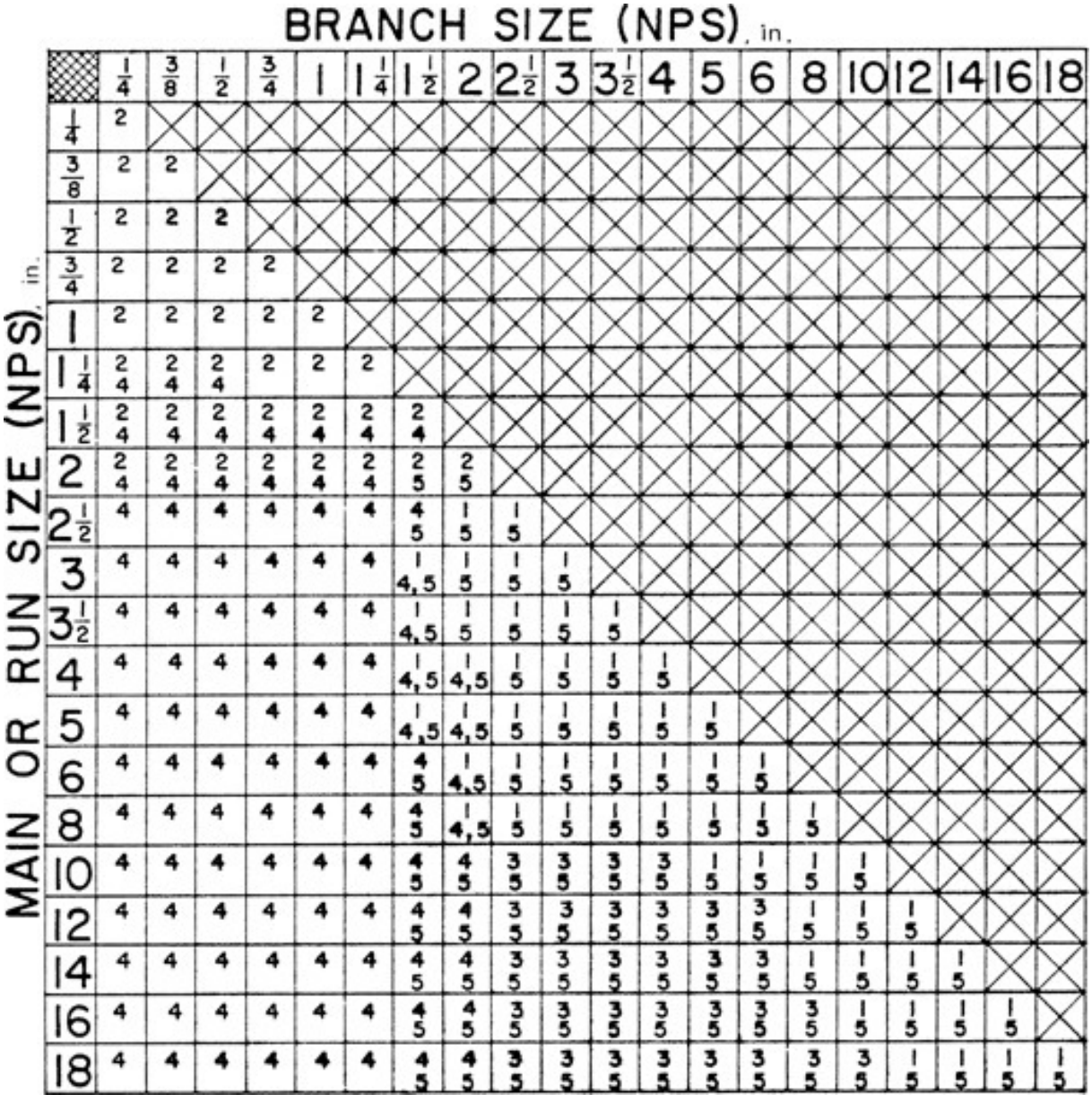

APPENDIX III: M.W. Kellogg chart

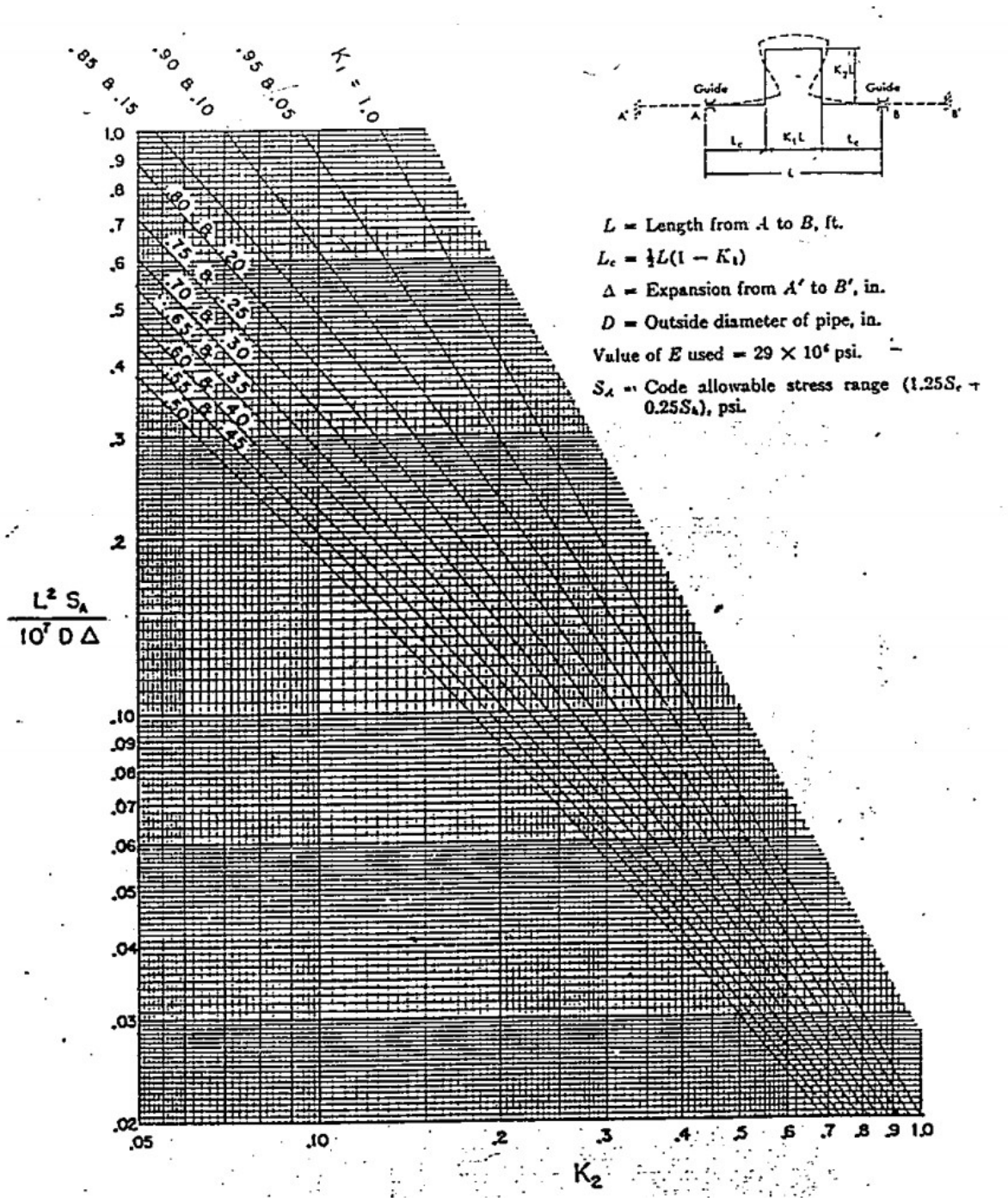

APPENDIX IV: EES model

```
{Demand analysis}
A_GSA=245000 {Greenhouse surface area}
T_ireqd=20 {Minimum required temperature inside greenhouse}
T_oreqd=8{ Minimum outside temperature}
Delta_Tgrhse=T_ireqd-T_oreqd
R_vcover=2 {Thermal resistance by air infiltration, greenhouse with plastic cover}
R_ocover=0.0873 {Thermal resistance by outside convection, at max air speed of 1.5 m/s}
R_lamdacover=0.01 {Thermal resistance by conduction, single plastic with 0.2 mm thickness}
R_icover=0.10 {Thermal resistance by inside convection, pipe installation below ceiling and on floor between plots}
R_kcover=R_ocover+R_lamdacover+R_icover{Overall thermal resistance}
Q_t=A_GSA*Delta_Tgrhse/R_kcover{Transmission losses through roof and walls}
Q_i=A_GSA*Delta_Tgrhse/R_vcover{ Infiltration losses}
Q_TotalD=Q_t+Q_i{Total heat losses/heating requirement}
V_dotD=Q_TotalD/(Rho_TD*C_pw*(T_3-T_9)){ Volume flow rate required at point D}
n_hsB=293
n_oc=6 {Assuming 6 occupants per house}
V_dotperperson=0.0000005 {BS 6700 recommendation}
rho_T11=Density(Water,T=T_11,x=0)
Q_RqdB=n_hsB*n_oc*V_dotperperson*(T_11-T_10)*C_pw*Rho_T11
V_dotB=Q_RqdB/(Rho_TB*C_pw*(T_3-T_9))
n_hsC=46
rho_T13=Density(Water,T=T_13,x=0)
Q_RqdC=n_hsC*n_oc*V_dotperperson*(T_13-T_12)*C_pw*Rho_T13
V_dotC=Q_RqdC/(Rho_TC*C_pw*(T_3-T_9))
n_hsE=57
n_ocE=2
rho_T17=Density(Water,T=T_17,x=0)
Q_RqdE=n_hsE*n_ocE*V_dotperperson*(T_17-T_16)*C_pw*Rho_T17
V_dotE=Q_RqdE/(Rho_TE*C_pw*(T_3-T_9))
Q_Total=Q_TotalD+Q_RqdB+Q_RqdC+Q_RqdE
V_dot=V_dotD+V_dotB+V_dotC+V_dotE{Volume flow rate from PS to A}

{Pipeline portion one- PS to Point A}
H_ps=2015"m"{pumping station altitude}
H_A=2211"m"{altitude at point A}
Delta_H1=H_A-H_ps"m"
L_pstoA=2400"m"{length of pipe segment from pumping station to point A}
T_fluid=150 "°C"
DN_1=0.210 {Taking DN 200}
DN_1=D_innxtstd
rho=Density(Water,T=T_fluid,x=0)
g=9.81 "m/s2"
P_design1=rho*g*Delta_H1

{Pipe thickness and mechanical stress analysis}
V_fluid=V_dot/(pi*(DN_1)^2/4)
D_o=0.219 "m"{Taking next std nominal pipe dia of 250mm}
E=0.85 {welding factor for arc weld buttweld}
y=0.4 {Temperature dependent coefficient for steels for <480oC}
R_m@T=340 "MPa"{Ultimate stress of steel S235}
R_p@50=235 "MPa"{Yield stress of steel S235 with fluid at 50oC}
R_p@200=185 "MPa"{Yield stress of steel S235 with fluid at 200oC}
R_p@150=R_p@50+(R_p@200-R_p@50)/(200-50)*(150-50) "MPa"{Yield stress of steel S235 with fluid at 150oC}
S_basic1=min(R_m@T/3,R_p@50/1.5,R_p@150/1.5) "MPa"{Basic allowable stress}
S_h1=min(R_m@T/3,R_p@150/1.5) "MPa"{Allowable stress hot}
A_thickness=0.0015 "m"{Assumed additional thickness for milling and corrosion}
t_m1=P_design1*D_o/(2*(S_basic1*1000000*E+P_design1*y))+A_thickness "m"{requested thickness}
```

t_n=0.0045 "m"{thickness}

{Length between supports}
t_e=0.050 "m"{Assumed insulation thickness}{confirm}
D_ins1=D_o+2*t_e"m"{insulation diameter}
rho_steel=7850 "kg/m3 "{Steel density}
rho_ins=830 "kg/m3 "{Insulation density}
C=0.6 {Form factor for pipe}
v_w=1.5 "m/s"{Maximum wind speed Naivasha}
e_factor=0.24 {Seismic factor}
q_p=pi*g*rho_steel*((D_o)^2-(D_innxtstd)^2)/4 "N/m"{Pipe weight}
q_e=pi*g*rho_ins*((D_ins1)^2-(D_o)^2)/4 "N/m"{insulation
weight}
q_sv=q_p+q_e"N/m"{Vertical sustained load}
q_w=pi*g*rho*((D_innxtstd)^2)/4 "N/m"{Water weight}
q_jv=0.5*e_factor*(q_w+q_p+q_e) "N/m"{Seismic vertical load}
q_ov=q_w+q_jv"N/m"{Vertical occassional/dynamic load}
q_wind=C*((v_w)^2)/1.6*D_ins1 "N/m"{Wind load}
q_sh=e_factor*(q_w+q_p+q_e) "N/m"{Seismic horizontal load}
q_oh=q_wind+q_sh"N/m"{Horizontal occassional load}
(L_s1)^2=((S_h1*1000000-P_design1*D_o/(4*t_m1))*(pi/4*((D_o)^4-
(D_innxtstd)^4))/(D_o*(q_sv+((q_ov)^2+(q_oh)^2)^0.5)))^0.5 "m"{Length between supports, load factor k
taken as 1, stress intensity factor 0.75i=1 for straight pipe}
Z=pi/32*(D_o^4-D_innxtstd^4)/D_o
M_A1=q_sv*(L_s1)^2/8 {Sustained bending moment}
M_B1=(q_ov^2+q_oh^2)^(1/2)*(L_s1)^2/8 {Occasional bending moment}
W_sust=P_design1*D_o/(4*t_m1)+M_A1/Z {Condition for sustained loads, W_sust<=kS_h1}
W_occas=W_sust+M_B1/Z {Condition for occasional loads, W_occas<=kS_h1}

{Pressure drop due to friction along the pipe}
mu=Viscosity(Water,T=T_fluid,x=0) {absolute viscosity}
R_e=rho*V_fluid*D_innxtstd/mu
eps=0.0005{roughness to cater for minor losses}
f=0.25/(log10((eps/D_innxtstd)/3.7+5.74/R_e^0.9))^2 {Friction factor}
n_b1=L_pstoA/60 {No. of bends}
n_v=2 {No. of valves}
n_u=0 {No. of T units}
n_c=0
h_b = 20*D_innxtstd{Equivalent length of bends}
h_c = 20*D_innxtstd
h_u = 20*D_innxtstd
h_v = 10*D_innxtstd
alpha=12.75*10^(-6) "1/°C"{Coefficient of thermal expansion for carbon steel at 150°C}
L_e=(L_pstoA+n_b1*h_b*D_innxtstd+n_c*h_c*D_innxtstd+n_u*h_u*D_innxtstd+n_v*h_v*D_innxtstd)
{Second equivalent length}
H_f=f*V_fluid^2*L_e/(2*g*D_innxtstd) {Head loss due to friction}
Delta_pdrop1=H_f*1000/L_pstoA{Pressure drop in mm/m}

{Pump power, pump station 1}
P_p=(Delta_H1+H_f)*rho*g "Pa"{Pump pressure}
eta_motor = lookup('Properties',2,'Column3')
eta_pump = lookup('Properties',1,'Column3')
eta=eta_motor*eta_pump
P=rho*g*(H_f+Delta_H1)*V_dot/eta/1000
P_ps1=P
L_brpipe=100 {Assumed}
p_inj=50 {Pressure in re-injection line is around 5 bar equivalent to 50m head}
rho_brine=Density(Water,T=T_2,x=0)
V_brine=(m_dotbrine/rho_brine)/(pi*(DN_1)^2/4) {velocity of return brine}
H_fbrpu=f*V_brine^2*L_brpipe/(2*g*D_innxtstd)
P_pbrnepu=H_fbrpu+p_inj{Brine pump pressure}
P_brpu=rho_brine*g*P_pbrnepu*(m_dotbrine/rho_brine)/eta/1000

```
P_brlne=P_brpu
c_p=lookup('Price table (Euro)',2,'Unit cost')
c_b=lookup('Price table (Euro)',3,'Unit cost')
c_cn=0
c_u=0
n_pu1=1
c_v=0
c_pu=lookup('Price table (Euro)',8,'Unit cost')
c_pu1=P_ps1*c_pu
c_pubrlne=P_brlne*c_pu
c_ins=lookup('Price table (Euro)',11,'Unit cost')
c_exptk=lookup('Price table (Euro)',12,'Unit cost')
c_pipelnepsA=(L_pstoA+L_connpipe+L_brpipe*2) *c_p + n_b1*c_b + n_c*c_cn + n_u*c_u +
n_v*c_v+L_pstoA*c_ins+V_exptank*c_exptk
c_ps1= n_pu1*c_pu1+c_pubrlne
c_hx1=A_s&t1*c_s&thx
C_c1=c_pipelnepsA+c_ps1+c_hx1
{Thermal expansion in pipes}
E_y=YoungsModulus(Carbon_steel, T=T_fluid) "Gpa"
T_cold=20
delta_T= T_fluid - T_cold
delta_L = alpha * L_pstoA* delta_T
epsilon_x = alpha/delta_T
Sigma_x = E_y*10^9 * epsilon_x
A_1 = pi*D_innxtstd*L_pstoA
F_a = A_1 * Sigma_x
{U_shape expansion loop}
Sc = min(R_m@T/3 , R_p@20/1.5 )
R_p@20=R_m@T+(R_p@50-R_m@T)/(50-0)*(20-0)
f_stress=0.3 {stress reduction factor for the maximum no. of displacement cycles ASME B31.3}
S_A=f_stress*(1.25*Sc + 0.25*S_h1)*1000000 {Allowable displacement stress range}
L_c=L_s1
K_1=0.5 {assumed}
L_c=1/2*L_x*(1-K_1)
Y_axis=(L_x)^2*S_A*0.000145038/10^7*D_o*delta_L{S_A converted to PSI for easy reference in the Kellogg
chart}
K_2=0.098 {As read from Kellogg chart}
W_loop=K_1*L_x
H_loop=K_2*L_x
L_loopbend=W_loop+2*H_loop{Total length of the U-expansion loop}
{Portion two- Point A to point D}
L_pstoD=5610 "m"
L_AtoD=L_pstoD-L_pstoA
L_bcB=1260
L_bcC=444
L_bcE=474
L_DtoR1=646
H_D=1946"masl"{altitude at point D}
Delta_H2=H_A-H_D
P_design2=rho*g*Delta_H2
n_b2=L_AtoD/60 {No. of bends}
n_u2=4 {No. of T units}
t_m2=P_design2*D_o/(2*(S_basic1*1000000*E+P_design2*y))+A_thickness "m"{requested thickness}
(L_s2)^2=((S_h1*1000000-P_design2*D_o/(4*t_m2))*(pi/4*((D_o)^4-
(D_innxtstd)^4))/(D_o*(q_sv+((q_ov)^2+(q_oh)^2)^0.5)))^0.5
L_e2=L_AtoD+n_b2*h_b*D_innxtstd+n_c*h_c*D_innxtstd+n_u2*h_u*D_innxtstd+n_v*h_v*D_innxtstd
H_f2=f*V_fluid^2*L_e2/(2*g*D_innxtstd)
Delta_pdrop2=H_f2*1000/L_AtoD{Pressure drop in mm/m}
c_bcp1=lookup('Price table (Euro)',6,'Unit cost')
```

c_bcp2=lookup('Price table (Euro)',7,'Unit cost')
c_s&thx=lookup('Price table (Euro)',10,'Unit cost')
c_pipelineAE=L_AtoD *c_p+L_bcB*c_bcp1+(L_bcC+L_bcE)*c_bcp2+n_b2*c_b + n_u2*c_u + n_v*c_v + L_AtoD*c_ins
c_hx2=A_s&tB*c_s&thx+A_s&tC*c_s&thx+A_s&tD*c_s&thx+A_s&tE*c_s&thx
C_c2=c_pipelineAE+c_hx2

{Return pipeline}
DN_9=DN_1
T_9=60
Rho_T9=Density(Water,T=T_9,x=0)
Delta_HDtoA=H_A-H_D
n_b3=(L_DtoA+L_Atops)/60
n_u3=0
n_v3=2
L_e3=L_Totalrtnmain+n_b3*h_b*D_innxtstd+n_c*h_c*D_innxtstd+n_u2*h_u*D_innxtstd+n_v3*h_v*D_innxtstd
H_f3=f*V_fluid^2*L_e3/(2*g*D_innxtstd)
Delta_pdrop3=H_f3*1000/(L_Totalrtnmain) {Pressure drop in mm/m}
P_pretrn=rho*g*(H_f3+Delta_HDtoA) {Pump pressure return line}
P_2=Rho_T9*g*(H_f3+Delta_HDtoA)*V_dot/eta/1000
P_ps2=P_2+P_R1
mu_R1=Viscosity(Water,T=T_9,x=0) {absolute viscosity}
DN_R1=0.0409 {DN 40}
V_R1=V_dotR1/((pi*DN_R1^2)/4) {Velocity of return pipe 1}
R_eR1=Rho_T9*V_R1*DN_R1/mu_R1
f_R1=0.25/(log10((eps/DN_R1)/3.7+5.74/R_eR1^0.9))^2 {Friction factor return pipe1}
V_dotR1=V_dotB+V_dotC+V_dotE
H_R1=1901
Delta_HDR1=H_D-H_R1
n_bR1=L_R1toD/60
n_vR1=1
L_eR1=L_R1toD+n_bR1*h_b*DN_R1+n_vR1*h_v*DN_R1
H_fR1=f_R1*V_R1^2*L_eR1/(2*g*DN_R1)
Delta_pdropR1=H_fR1*1000/(L_R1toD) {Pressure drop in mm/m return line 1}
P_pretrnR1=Rho_T9*g*(H_fR1+Delta_HDR1) {Pump pressure return line 1}
P_R1=Rho_T9*g*(H_fR1+Delta_HDR1)*V_dotR1/eta/1000 {Pump power for return line return line 1}
L_R1toD=L_DtoR1
L_bcEr=L_bcE
L_DtoA=L_AtoD
L_bcCr=L_bcC
L_bcBr=1770
L_Atops=L_pstoA
L_Totalrtnmain=L_DtoA+L_Atops
L_Totalrtnbrcn1=L_bcBr{DN 100 pipe}
L_Totalrtnbrcn2=L_bcCr+L_bcEr{DN 65 pipe}
c_R1p=lookup('Price table (Euro)',13,'Unit cost')
n_pu2=1
c_pu2=P_ps2*c_pu
c_pipelineR=L_Totalrtnmain*c_p+L_Totalrtnbrcn1*c_bcp1+L_Totalrtnbrcn2*c_bcp2+L_R1toD*c_R1p
c_ps2=n_pu2*c_pu2
C_c3=c_pipelineR+c_ps2

{Shell and tube heat exchanger, ps1}
LMTD_ps1=((T_fluid-T_3)-(T_2-T_9))/ln((T_fluid-T_3)/(T_2-T_9))
U_o=1190 "W/m2 oC"{Overall duty heat transfer coefficient from process engineering hand book}
C_pw=4180
T_2=90
Delta_Tbrine=T_fluid-T_2
m_dottonphr=238
m_dotbrine=m_dottonphr/3.6

```
Q_brine=(m_dotbrine*C_pw*Delta_Tbrine)/1000000 "Mw"
A_s&t1=Q_brine*1000000/(U_o*LMTD_ps1) {Outside area of metal surface through which heat is exchanged}

{Shell and tube heat exchanger, point B}
T_11=60
T_5=T_9
T_10=15
LMTD_B=((T_3-T_11)-(T_5-T_10))/ln((T_3-T_11)/(T_5-T_10))
Delta_TB=T_3-T_5
rho_TB=Density(Water,T=T_3,x=0)
m_dotB=V_dotB*rho_TB
A_s&tB=Q_RqdB/(U_o*LMTD_B)

{Shell and tube heat exchanger, point C}
T_13=T_11
T_6=T_9
T_12=T_10
LMTD_C=((T_3-T_13)-(T_6-T_12))/ln((T_3-T_13)/(T_6-T_12))
Delta_TC=Delta_TB
rho_TC=rho_TB
m_dotC=V_dotC*rho_TC
A_s&tC=Q_RqdC/(U_o*LMTD_C)

{Shell and tube heat exchanger, point D}
T_14=20
T_15=T_11
T_7=T_9
LMTD_D=((T_3-T_15)-(T_7-T_14))/ln((T_3-T_15)/(T_7-T_14))
Delta_TD=Delta_TB
rho_TD=rho_TB
m_dotD=V_dotD*rho_TD
A_s&tD=Q_TotalD/(U_o*LMTD_D)

{Shell and tube heat exchanger, point E}
T_8=T_9
T_17=T_11
T_16=T_10
LMTD_E=((T_3-T_17)-(T_8-T_16))/ln((T_3-T_17)/(T_8-T_16))
Delta_TE=Delta_TB
rho_TE=rho_TB
m_dotE=V_dotE*rho_TE
A_s&tE=Q_RqdE/(U_o*LMTD_E)
A_hxtotal=A_s&t1+A_s&tB+A_s&tC+A_s&tD+A_s&tE

{Branch connections}
DN_51=0.1053{From ASTM F681 – 82 (2008) Standard Practice for Use of Branch Connections. Fabricated
joint (cut-in branch)}
DN_51o=0.114
DN_52=DN_51
DN_10=DN_52 {Assumed}
DN_11=DN_10
DN_61=0.064 {From ASTM F681 – 82 (2008) Standard Practice for Use of Branch Connections. Fabricated
joint (cut-in branch)}
DN_62=DN_61
DN_12=DN_62 {Assumed}
DN_13=DN_12
DN_71=DN_1
DN_72=DN_71
DN_14=DN_71
DN_15=DN_14
DN_81=DN_61
DN_82=DN_81
DN_16=DN_81
```

```
DN_17=DN_16
Beta=60
d_1bc=(DN_51-2*(t_n-A_thickness))/sin(Beta) {Effective length removed from pipe at branch}
d_2bc=(t_n-A_thickness)+(t_n-A_thickness)+d_1bc/2 {d_2bc=d_1bc because d_1bc >calculated d_2bc}{Half width of reinforcement zone}
L_41=2.5*(t_n-A_thickness)
T_r=t_n
L_42=2.5*(t_n-A_thickness)+T_r
L_4=L_42 {Height of reinforcement zone outside of run pipe}
A_rf=t_m2*d_1bc*(2-sin(Beta)) {Required reinforcement area}

{Expansion tank, point A}
L_connpipe=457
T_3=145
rho_coldw=1000
r_pipe1=DN_1/2
r_pipe2=DN_51/2
r_pipe3=DN_61/2
h_pipe1=L_pstoA*2+L_AtoD*2
h_pipe2=L_bcB+L_bcBr+L_bcCr
h_pipe3=L_DtoR1+L_bcE+L_bcC+L_bcEr+L_R1toD
V_pipe1=pi*r_pipe1^2*h_pipe1
V_pipe2=pi*r_pipe2^2*h_pipe2
V_pipe3=pi*r_pipe3^2*h_pipe3
V_pipe=V_pipe1+V_pipe2+V_pipe3
rho_T3=Density(Water,T=T_3,x=0)
V_heatedh2o=V_pipe*rho_coldw/rho_T3
V_exptank=V_heatedh2o-V_pipe

{capital cost}
c_unc=lookup('Properties',8,'Column3') {cost of uncertainity}
c_d&sup=lookup('Properties',9,'Column3') {cost of design and supervision}
c_pipelineTotal=c_pipelnepsA+c_pipelineAE+c_pipelineR
c_psTotal=c_ps1+c_ps2
c_hxTotal=c_hx1+c_hx2
c_addtn=(C_c1+C_c2+C_c3)*(c_unc+c_d&sup)
C_cTotal=C_c1+C_c2+C_c3+c_addtn

{Annual cost}
c_elunit=lookup('Properties',4,'Column3') {USD/Kwh from LCPDP of Kenya}
o_h=lookup('Properties',7,'Column3')
P_Tpp=P_ps1+P_ps2+P_brlne
PMT=C_cTotal/((1-1/(1+i)^N)/i)
c_pu&movingparts=0.10*c_psTotal
c_pscivil&piping=c_psTotal-c_pu&movingparts
c_o&mpu&movingparts=0.04*c_pu&movingparts
c_o&mpscivil&piping=0.01*c_pscivil&piping
c_o&mhx=0.02*c_hxTotal
c_o&mpipeline=0.01*c_pipelineTotal
c_o&maintTotal=c_o&mpu&movingparts+c_o&mpscivil&piping+c_o&mhx+c_o&mpipeline {O&M assumed 4% for pumps and moving parts, 1% for pump stations civil structures and piping, 2% for Hxs and 1% for rest of pipeline}
C_elect=c_elunit*0.77*o_h*P_Tpp
C_a=PMT+c_o&maintTotal+C_elect

{Total updated cost, C_T}
i=lookup('Properties',6,'Column3')
N=lookup('Properties',5,'Column3')
C_T=C_cTotal+C_a/i*(1-1/(1+i)^N) {i& N assumed as 6% and 30 yrs}

{Unit production cost of heat}
P_heat=Q_brine*1000*o_h
c_heat=(C_a/P_heat)*1000 {Euro/MWh}
```